UNIVERZA V LJUBLJANI
FAKULTETA ZA FARMACIJO

VERONIKA ROŽMAN

MAGISTRSKA NALOGA

RAZVOJ BIORAZGRADLJIVIH POLIMERNIH FILMOV Z NANOSTRUKTURIRANO POVRŠINO

UNIVERZITETNI ŠTUDIJ INDUSTRIJSKE FARMACIJE

Ljubljana, 2018

UNIVERZA V LJUBLJANI
FAKULTETA ZA FARMACIJO

VERONIKA ROŽMAN

MAGISTRSKA NALOGA

RAZVOJ BIORAZGRADLJIVIH POLIMERNIH FILMOV Z NANOSTRUKTURIRANO POVRŠINO

DEVELOPMENT OF BIODEGRADABLE POLYMER FILMS WITH NANOSTRUCTURED SURFACE

UNIVERZITETNI ŠTUDIJ INDUSTRIJSKE FARMACIJE

Ljubljana, 2018

The experimental work was carried out at Marmara University in Istanbul, Turkey at the Department of Pharmaceutical Technology.

The project was funded by Erasmus exchange programme and additionally by TUBITAK (The Scientific and Technological Research Council of Turkey) with the grant number 114S525.

Iskreno se zahvaljujem izr. prof. dr. Petri Kocbek, da me je sprejela pod svoje mentorstvo, mi strokovno svetovala in spodbujala pri nastajanju magistrske naloge. Potrpežljivo me je vodila v pravo smer in bila vedno na voljo, ko sem jo potrebovala.

Special thanks to co-mentor assis. prof. dr. Gökçen Yaşayan, who inspired me with her broad knowledge for the topic of nanotopography. She created a very pleasant environment to work in and guided me professionally through the whole master research thesis. I am truly thankful for being able to work with her.

Iz srca sem hvaležna mami in očetu, da sta mi študij omogočila in me tekom izobraževanja nenehno podpirala.

Izjava

Izjavljam, da sem magistrsko nalogo izdelala samostojno, pod mentorstvom izr. prof. dr. Petre Kocbek in somentorstvom doc. dr. Gökçen Yaşayan.

Veronika Rožman

Predsednik komisije:

Izr. prof. dr. Mitja Kos

Mentorica:

Izr. prof. dr. Petra Kocbek

Somentorica:

Doc. dr. Gökçen Yaşayan

Član komisije:

Doc. dr. Matej Sova

CONTENT

ABSTRACT

Cell response to nanoscale feature dimensions and shape has been largely investigated for the last decades. At the nano level, the surface area per weight unit of material is larger therefore a potential for interactions is higher. There are several studies demonstrating that nanostructured surfaces affect cell adhesion, migration, morphology, proliferation and gene expression. These findings can be useful in designing new drug delivery systems, implants and tissue engineering scaffolds.

Methods for nanostructuring can be divided to "top down" and "bottom up" methods, depending on whether nanofeatures are shaped out of bulk material or made with the help of interactions between primary building blocks (atoms, molecules). Final structures are usually two-dimensional, however there are methods to design three-dimensional models as well.

To analyze nanostructured surfaces different techniques can be used such as contact angle measurements, scanning electron microscopy and atomic force microscopy. With the latter, the preparation of a sample for imaging is not demanding and almost any material surface can be imaged in air or liquid conditions.

In this study, we combined colloidal lithography, nanosphere soft lithography and polymer casting method to create hexagonal shaped nanofeatures on the surface of biodegradable polymer film. We created polystyrene templates with nanospheres in diameters of 27 nm, 62 nm, 99 nm, 210 nm and 280 nm transferred to the silicon wafer cut surfaces. Smooth silicon wafer cut served as a blank. A negative relief mold was made by curing the polydimethylsiloxane elastomer on top of the templates. At the end, polycaprolactone solution in chloroform was poured into the mold, left to dry and transform to the film.

Polystyrene templates, polydimethylsiloxane molds and polycaprolactone films were analyzed by atomic force microscopy. The smallest feature diameter topography which was successfully transferred from the template to the film was 99 nm. With 27 nm and 62 nm features nanostructured surfaces could not be created due to multilayer nanoparticle formation and thus disruption of the surface topography. 210 nm and 280 nm features showed high accuracy without any disruptions in the surface topography.

We have confirmed that the method used is appropriate for nanostructuring of polymer materials. Cell culture response to nanotopography should be investigated in detail in the

future studies to confirm the advantages of nanostructured surfaces in the area of biomedicine.

POVZETEK

Beseda topografija izhaja iz grških besed ‘topos’, ki pomeni prostor, in ‘graphia’, ki pomeni pisati. Nanotopografijo zunajceličnega okolja lahko opišemo kot razporeditev strukturnih elementov (višina, dolžina in širina struktur, medsebojna oddaljenost struktur ipd.) na površini, s katero je celica v stiku. Velikost topografskih elementov je manjša od 1 μm, bolj natančno, manjša ali enaka 100 nm.

Glede na topografijo lahko nanostrukturirane površine razdelimo na tiste z neprekinjeno in tiste s prekinjeno topografijo. Le-ti se naprej delita glede na usmerjenost strukturnih elementov na anizotropno in izotropno; ter sekundarno, glede na spremembe osnovnih topografskih elementov, na enotno (homogeno) ali stopenjsko.

Nanostrukturirana površina, ki je v stiku s celicami, vpliva na njihov odziv in nadaljnji razvoj. Na nanometrskem nivoju je stična površina, ki je na voljo za interakcije večja, posledično je večje tudi število možnih stičnih mest s celicami. Nanostrukturiranost površine vpliva na adhezijo, migracijo, morfologijo in proliferacijo celic ter izražanje celičnih genov. Najpogosteje prisotne strukture nanometrskih velikosti v biološkem okolju so izbokline, žlebi in jamice. Poleg oblik strukturnih elementov na odziv celic močno vplivajo tudi dimenzije topografskih struktur. Razvoj biorazgradljivih materialov z nanostrukturirano površino, ki vplivajo na celični odziv, lahko pripomore k nadzorovani dostavi učinkovin, omogoči pripravo implantatov in nosilcev v tkivnem inženirstvu.

Topografija površine je poleg kemijske sestave in elastičnosti substrata ena glavnih lastnosti, ki vplivajo na odziv celice. To je leta 1914 ugotovil ameriški biolog R. G. Harrison, ko je med gojenjem fibroblastov, ki jih je izoliral iz živčnega sistema embrijev žab, na pajkovi mreži opazil, da so le-ti prilagodili svojo obliko po poteku niti v mreži. V naslednjih desetletjih je sledilo veliko podobnih odkritij, ki so vplivala na razvoj metod za mikro- in kasneje tudi nanostrukturiranje površin.

Celice se odzivajo na notranje in zunanje signale, ki jih pridobijo preko interakcij z drugimi celicami in zunajceličnim ogrodjem. Zunajcelično ogrodje vsakega tkiva ima specifično nanostrukturirano površino, kjer so interakcije in z njimi povezane signalne poti

zelo kompleksne, zato vpliv zunajceličnega ogrodja na celice *in vivo* še ni popolnoma znan. Najbolj raziskan proces je aktivacija α- in β-verig transmembranskih proteinov t.i. integrinov. Integrinski receptorji se specifično vežejo na strukture zunajceličnega ogrodja in skupaj z adaptorskimi proteini, kot sta talin in vankulin, tvorijo komplekse oz. fokalne adhezije. Fokalne adhezije neposredno vplivajo na citoskelet, strukturo in obliko celic. V fokalne adhezije so vključeni tudi signalni proteini, kot je paksilin, ki sprožajo biokemijske signalne kaskade, ki sodelujejo pri transkripciji, proliferaciji in diferenciaciji celic.

Adhezija celic na zunajcelično ogrodje poteka preko transmembranskih receptorjev, najpogosteje integrinov, in je najpomembnejša stopnja razvoja, brez katere celica podleže apoptozi (programirani celični smrti). Nanotopografija lahko spodbudi ali prepreči celično adhezijo. Na uspešnost interakcij v večji meri kot oblika nanostruktur vplivajo njihove dimenzije. Večina celic se pritrdi na nanostrukture točno določene velikosti in oblike, jakost adhezije pa se drastično zmanjša pri velikostih, ki so pod ali nad to specifično velikostjo.

Nanotopografija vpliva tudi na morfologijo in orientacijo različnih vrst celic. Sprememba morfologije se največkrat kaže tako, da celice postanejo manjše, okrogle, citoskelet pa manj organiziran. Stopnja orientacije je najbolj odvisna od vrste celic, globine in širine topografskih elementov.

Proliferacijski odziv celic na nanostrukturirane površine je zelo raznolik. Odvisen je od vrste celic in oblike nanostrukturnih elementov. Najpogostejši odziv je zmanjšana sposobnost celične proliferacije, znani pa so tudi primeri povečane proliferacije določenih vrst celic.

Na celice *in vivo* vplivajo fizični, mehanski in kemijski dražljaji iz okolja. Vsi dražljaji skupaj povzročijo sinergistične ali antagonistične učinke na celico. Za razumevanje vpliva mikrookolja na celice in njihov razvoj, je zato potrebna ocena skupnega učinka vseh dražljajev, kar ni enostavno, saj je celični odziv na fizične dražljaje velikokrat odvisen tudi od celičnega fenotipa.

Večina metod za nanostrukturiranje površin izhaja iz industrije elektronike. Pri vsaki metodi, ki omogoča nanostrukturiranje površin, je pomembno, da je ta ponovljiva, da omogoča sočasno strukturiranje čim večje površine in da jo je mogoče izvesti tudi brez uporabe zahtevne opreme. Glede na pristop k izdelavi nanostrukturiranih površin metode nanostrukturiranja delimo na "od zgoraj navzdol" (ang. "top-down") in "od spodaj navzgor" (ang. "bottom-up"), glede na končno nanostrukturo površine pa na 2D in 3D

metode. Osnova metod "od zgoraj navzdol" je material, katerega površina se nato oblikuje - nanostrukturira. Nasprotno, se pri metodah "od spodaj navzgor" začne strukturiranje površine z načrtovanjem interakcij med atomi, molekulami ali delci, ki se sami združijo ali samoorganizirajo v višje kompleksne nanostrukture.

Za razvoj modelov nanostrukturiranih površin uporabljamo najrazličnejše materiale, od sinteznih polimerov, kot so polipropilen in polikaprolakton, do naravnih polimerov, kot sta želatina in hitosan, pa tudi kovine npr. zlato.

Najpogostejše tehnike za analizo nanostrukturiranih površin so: merjenje stičnih kotov za določanje hidrofilnosti/hidrofobnosti, vrstična elektronska mikroskopija, vrstična tunelska mikroskopija in mikroskopija na atomsko silo. Slednja omogoča enostavno pripravo in podrobno analizo vzorca tako v zraku kot v tekočini.

V nalogi smo se osredotočili na razvoj nanostrukturiranih biorazgradljivih polimernih filmov iz polikaprolaktona z velikostjo sferičnih strukturnih elementov 27 nm, 62 nm, 99 nm, 210 nm in 280 nm. S takšnimi nanostrukturiranimi filmi želimo vplivati na adhezijo in razvoj celic v telesu in jih tako uporabiti za regeneracijo tkiv. Metodo nanostrukturiranja biorazgradljivih filmov, ki smo jo uporabili v naši raziskavi, je začela razvijati dr. Yaşayan. Za izdelavo nanostrukturiranih filmov je uporabila biorazgradljiv kopolimer mlečne in glikolne kisline.

Predlogo za nanostrukturiranje površine smo ustvarili s prenosom polistirenskih nanosfer na gladko površino silicijevih ploščic. Silicijeve plošče smo na začetku razrezali na manjše ploščice (1.5 x 1.5 cm^2) in jih očistili v ultrazvočni kopeli in v UV/Ozone ProCleaner™ Plus, hkrati smo na ta način povečali hidrofilnost površine, ki je potrebna za prenos nanosfer iz vodne površine na silicijevo ploščico. Za izdelavo predlog na površini silicijevih ploščic smo uporabili polistirenske sfere velikosti 27 nm, 62 nm, 99 nm, 210 nm in 280 nm. Etanolno suspenzijo polistirenskih sfer smo s kapalko nanesli na vodno površino (Milli-Q voda) v petrijevki. Pri enakomerni ureditvi sfer na površini vode smo si pomagali z raztopino natrijevega dodecilsulfata. Polistirenske sfere smo prenesli na silicijeve ploščice tako, da smo vsako ploščico pod kotom potopili v vodo in previdno privzdignili sloj nanosfer iz površine. Za kontrolo smo uporabili zgolj silicijevo ploščico brez polistirenskih nanosfer (gladka površina).

Kalupe smo izdelali po postopku mehke litografije. Na pripravljene polistirenske predloge različnih dimenzij (27 nm, 62 nm, 99 nm, 210 nm, 280 nm) smo počasi vlili polidimetilsiloksan in s tem ustvarili negativni relief nanostrukturirane površine v

elastomer. Izdelane kalupe smo čez noč pustili v vakuumski pečici, da smo odstranili ujete mehurčke zraka, nato pa še dodatno pospešili strjevanje v sušilni komori. Po končani izdelavi smo z acetonom odstranili preostale polistirenske sfere in ostale možne nečistoče. Z mikroskopijo na atomsko silo smo posneli površine vseh polistirenskih predlog in polidimetilsiloksanskih kalupov. Polistirenske predloge dimenzij 27 nm in 62 nm in njihovi odgovarjajoči kalupi so pri analizi z mikroskopom na atomsko silo pokazali razgibano, nerazločno topografijo. Na podlagi teh ugotovitev smo nadaljevali izdelavo polikaprolaktonskih filmov z nanostrukturami velikosti 99 nm, 210 nm in 280 nm in kontrolnih nestrukturiranih filmov.

Razvoj polikaprolaktonskih filmov je zaradi uporabe kloroforma v formulaciji potekal v laminarni komori. V silikonske kalupe smo previdno vlili tekočo formulacijo polikaprolaktona v kloroformu. Ko je kloroform popolnoma izhlapel, je v kalupu nastal tanek rigiden film z nanostrukturirano površino.

Najmanjša dimenzija nanostruktur na površini polimernega filma, pri kateri smo z mikroskopijo na atomsko silo uspeli dokazati enakomerno razporeditev struktur na površini, je bila 99 nm, vendar smo na polistirenskem modelu kot v primeru manjših dimenzij struktur na površini opazili območja večplastnosti in prekinitev, ki so se preko kalupa projicirala na polikaprolaktonski film. Rezultati raziskave dr. Yaşayan s poli(D, L-mlečno-ko-glikolno) kislino so bili zelo podobni, saj je bila najmanjša dimenzija struktur, s katero so dosegli enakomerno razporeditev topografskih struktur, prav tako 99 nm. Analiza polistirenskih predlog s strukturami velikosti 210 nm in 280 nm je pokazala, da je struktura površine predlog brez motenj. Strukturne značilnosti predloge so se uspešno prenesle na polidimetilsiloksanski kalup in polikaprolaktonski film, ki je imel natančno ureditev topografskih elementov brez prekinitev.

V preliminarne raziskave celičnega odziva na nanostrukturirane polikaprolaktonske filme smo vključili tiste z velikostjo strukturnih elementov 99 nm, 210 nm, 280 nm ter kontrolne filme. Za preizkus smo uporabili štiri plošče za gojenje celic s 24 vdolbinami. Napolnili smo jih do tretjine s polidimetilsiloksanom. V vsako vdolbino smo nato s pomočjo igle za brizgo pritrdili polikaprolaktonske filme z nanostrukturirano površino obrnjeno navzgor. Tako pripravljene gojitvene plošče s filmi z nanostrukturirano površino smo ustrezno površinsko sterilizirali pod UV svetlobo in poslali na zunanji inštitut tj. Oddelek za biofiziko Univerze Marmara, da bi ovrednotili živost celic ob stiku z nanostrukturirano površino. Zaradi fiksiranja filmov z iglami so se filmi ob stiku z medijem za gojenje celic

upognili, kar je onemogočilo izvedbo eksperimenta. Obstaja možnost, da so se celice pritrdile na nanostrukturirano površino filmov, vendar zaradi upognjenosti filma tega ni bilo mogoče dokazati.

Na podlagi dobljenih rezultatov lahko zaključimo, da je uporabljena metoda za izdelavo nanostrukturiranih filmov ponovljiva na različnih biopolimerih. Minimalna velikost strukturnih elementov je 99 nm, kar velja za našo raziskavo in literaturne podatke, da dosežemo enakomerno strukturiranost površine polimernega filma; vendar se lahko tudi pri tej dimenziji pojavijo lokalno večplastne strukture in prekinitve homogene nanostrukturiranosti površine. Pri dimenzijah strukturnih elementov 210 nm, 280 nm in več, lahko s to metodo izdelamo nanostrukturirane filme z visoko stopnjo strukturne urejenosti brez prekinitev nanostrukturiranosti površine. Za testiranje celičnega odziva na nanostrukturirane filme je potrebno razviti metodo ustrezne priprave filmov, ki bo preprečila zvijanje filmov ob stiku z medijem.

LIST OF ABBREVIATIONS

- ECM – extracellular matrix
- PLGA – poly (lactic-co-glycolic acid)
- PDMS – polydimethylsiloxane
- AFM – atomic force microscopy
- PCL – polycaprolactone
- PS – polystyrene
- DPN – dip pen nanolithography
- PVD – physical vapor deposition
- CVD – chemical vapor deposition
- STM – scanning tunneling microscopy
- SEM – scanning electron microscopy
- SDS – sodium dodecyl sulfate

1. INTRODUCTION

1.1. Nanotopography

Materials for biomedical applications should be designed considering their surface properties, since cells, being normally micrometer sized, can respond to nanotopography of growth surface. The extracellular matrix (ECM), which surrounds cells, represents environment through which cells receive biochemical and biophysical cues. It is built from nanosized building blocks (1). In the last decades, many studies showed that surface features of materials on the nanoscale level influence cell adhesion, cytoskeletal arrangement, migration, proliferation, expression of genes, intercellular communication, ECM formation, differentiation and the way the cells respond to extracellular signals (2). This opened a possibility to design substrate surface nanotopography and thus mimic structure of the ECM *in vivo* (1).

When biomaterials are produced it is likely that nanotopography is created on the surface of the material, either deliberately or by accident. Even macroscopically flat materials are likely to have topography of a few nanometers, but this may be insufficient to induce cell response (2). To determine minimal nanometer sized surface topography to which cells respond is difficult, considering different cell types and different substrate materials, which differ in substrate porosities, geometry and size of the features, and their surface density (3). There are some studies that claim cell response down to 13 nm sized feature dimension (4).

Compared to micrometer sized surface topographies, nanosurfaces have unique properties and surface energy due to higher surface area, higher surface roughness and higher numbers of defects in surface structure (5). Based on this knowledge, novel nanostructured biomedical applications are being developed in the field of cell culture, diagnostics, drug delivery, regenerative medicine, medical imaging, cancer therapy and gene therapy. Such materials with nanostructured surfaces include e.g. diagnostic tests for detection of microbes *in vitro*, biosensors, tissue engineering scaffolds, materials for dental application, resorbable sutures, bone screws and drug delivery devices, wound dressings, imaging contrast agents and cancer diagnostic tools (6, 7).

1.2. History of surface patterning

The first indications that topography of the growth surface influences cell response appeared in 1914 when R. G. Harrison investigated fibroblasts isolated from the embryonic nervous tissue of frogs. Fibroblasts adopted stretched morphology on the spider silk web (8). In 1934, Weiss *et al.* made similar observation with embryonic chicken spinal neurons. They described the phenomenon of cell response to surface characteristics of their microenvironment as 'contact guidance' (9). After many experiments, Weiss and colleagues also proved that neuronal cells adhere, elongate, and migrate on glass surface along fibers with diameter from 10 to 30 μm (10).

Later, in 1964, Curtis and Varde researched response of fibroblasts from the heart of a chicken on different surface topographies (11). They concluded that cells respond to cell density in culture as well as to the topography of their microenvironment (10).

In 1977 Jenkins *et al.* used one of the first commercial carbon fibers to sew up a fractured ligament (12). The cells migrated along the fiber and rebuilt a tendon.

Various micro- and nanofabrication methods have been developed and numerous studies made to prove that many cell types respond strongly to surface topography. Recent methods of surfaces patterning are most widely used in the microelectronic industry (1). Photolithography was introduced into semiconductor industry in 1970, and into biology in 1988 by Kleinfeld *et al* (13). A. Formhals patented electrospinning in 1934 (14). Its adaptation for application in biomedical engineering was made in the early 2000s, when the first biodegradable materials were electrospun. (15). Soft lithography was introduced into biomedical applications in 1990s by George Whitesides with flexible polydimethylsiloxane (PDMS) molds (16).

1.3. Complex ECM organization

Cell behavior is determined via intrinsic and extrinsic cell signals resulting from intercellular interactions and interactions of cells with ECM (3). The ECM is a complex network of protein fibers ranging from 10 nm to 300 nm in diameter such as collagen, elastin, proteoglycans and glycoproteins (17). Its composition and structure depend on the cell phenotype and the function of specific tissue (18). For example, the ECM in dermis is a network of organized fibers 30-130 nm in diameter (19). Bone tissue ECM exhibits characteristic nanotopography with its hierarchically organized structure, composed mostly

of collagen type I, which is secreted by bone cells (18). In the myocardium, the ECM is composed of aligned fibrils approximately 100 nm in diameter. The cells are parallelly ordered according to the direction of fibrils (20).

Understanding ECM arrangement and the impact of ECM on cells *in vivo* is demanding due to the small scale on which the interactions occur, various physico-chemical signals present and structural differences in various types of tissues, having specific and distinct ECM composition and organization (18).

1.4. Classification of nanotopographies

The term topography comes from the Greek words ‘topos’ – place and ‘graphia’ – writing (21). Topography can be described as the study and the description of the distribution of physical features on the surface (22). The term ‘nano’ usually refers to dimensions less than 1 μm, or more specifically less than or equal to 100 nm in at least one dimension (23). Various shapes of nanofeatured surfaces such as beads, circles, pores, wells, steps, pillars, grooves, pits, fibers, circles and many more are described in the literature (3). The most common features in natural tissues, are however, nanoprotrusions, nanopits and nanogrooves. Nanoprotrusions appear within the ECM of various tissues, while nanopits appear in the aortic valve in the heart, basement membrane of the cornea and in the circulatory system. Nanogrooves resemble the natural state of many cell type surfaces *in vivo* such as surfaces of fibroblasts, osteoblasts, nerve cells, and mesenchymal stem cells so they can directly affect cellular alignment through contact guidance (24).

Topographies can be categorized as continuous and discontinuous (Fig. 1).

a)

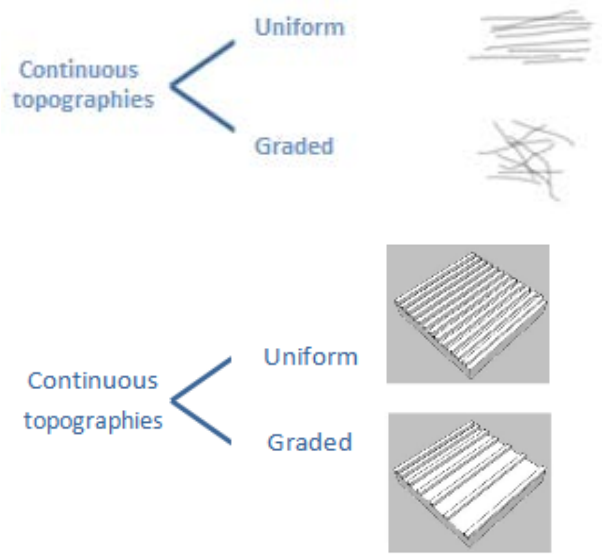

b)

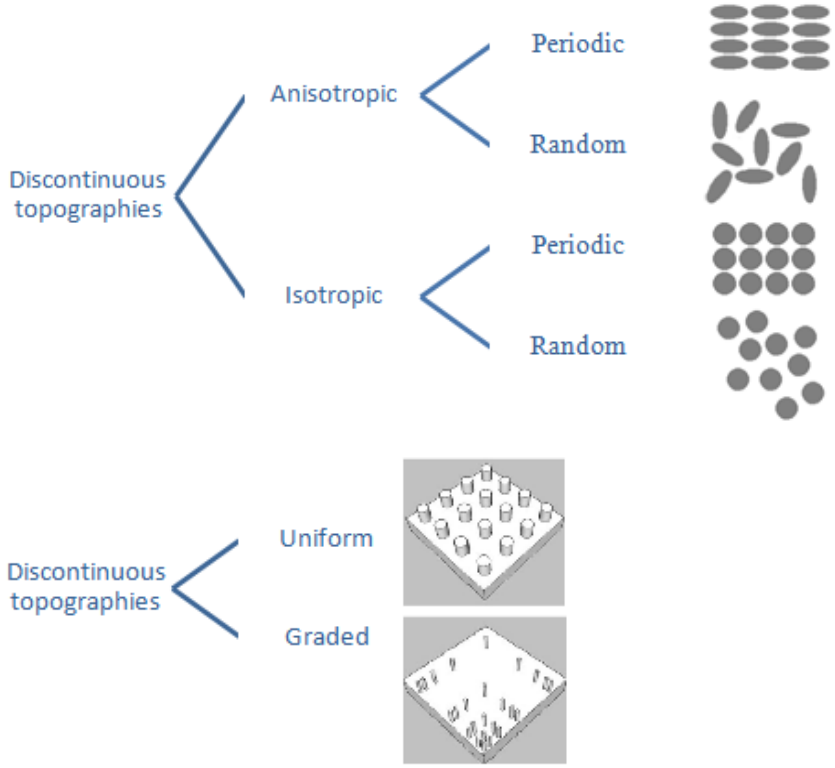

Fig. 1: An example of topography classification. (a) According to the direction of structural elements continuous topographies can be divided to anisotropic and isotropic and according to uniformity to uniform and graded. (b) Discontinuous topographies can be distinguished by asymmetry as anisotropic and isotropic and by uniformity as uniform and graded. Adapted from reference (25).

Continuous topographies are divided according to direction to anisotropic, which are oriented along a single axis (e.g. parallel oriented fibers), and isotropic, which are oriented along many different axes (e.g. random oriented fibers) (Fig. 1a). Discontinuous topographies are divided according to the symmetry of the features to isotropic which are symmetric features (e.g. circular pillars), and anisotropic which are asymmetric features (e.g. elliptical pillars) (Fig. 1b). If the distribution of the discontinuous features is considered, they can also be divided to periodic and random. If the features are consistent both continuous and discontinuous topographies are uniform and if there appear to be gradual changes in the features they are considered as graded (25).

1.5. Cell response to substrate nanotopography

Cells may encounter macrotopography, like bone or ligament tissue, microtopography, such as the shapes of other cells and nanotopography, like protein folding and collagen fibrils (26). Cells can response to very small nanotopographical features. Epithelial and endothelial cells respond to depths of 70 nm (2). Macrophages respond to surface structures down to 30 nm (27). Fibroblasts respond to the surface structures as small as 13 nm (4). Some cell types exhibit similar response, while others completely different response to the same topography. Even, when the cell response is similar, cells can exhibit different sensitivities to the nanostructures, demonstrated as stronger/weaker or quicker/slower cell responses (7).

Cells can sense topography of environment and than create focal adhesions via filopodia, which dimensions are in the nanometre range (250-400 nm) (28). Fibroblasts have been described to sense and align to microgrooves via their filopodia (29). Macrophages have been reported to sense grooves down to a depth of 71 nm by active formation of filopodia and their elongation in response to the shallow topography (30).

The other mechanism of cells responding to topography is through activation of α- and β-chain transmembrane proteins, i.e. integrins (Fig. 2) (24). These receptors bind to ECM and form focal adhesions containing adaptor proteins like talin and vinculin that can directly affect cell structure, shape and cytoskeletal arrangement. They also contain signaling proteins, like paxillin, which initiates biochemical signaling, resulting in changes in cell transcription, proliferation and differentiation (25).

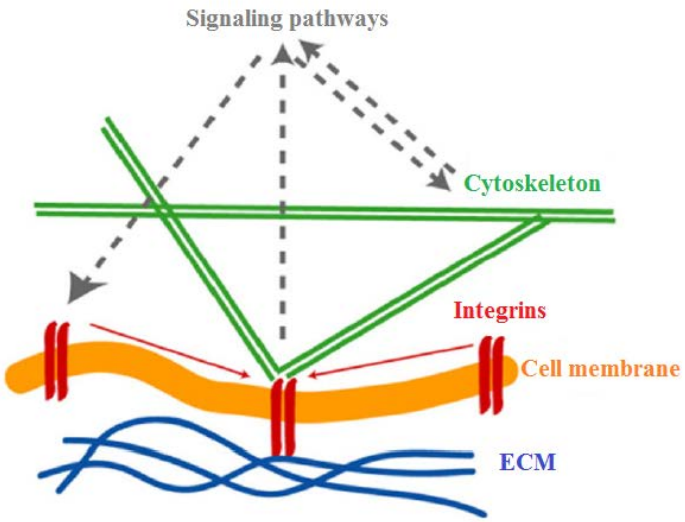

Fig. 2: Simplified presentation of arrangement of focal adhesion complex. Integrins connect to ECM ligands on the outside of the cell surface and to cytoskeleton on the inside of the cell. Adapted from reference (31).

1.5.1. Effects of nanotopography on cell adhesion

To migrate, proliferate and differentiate, most cells need to adhere to their ECM. If the cell does not attach, it eventually undergoes apoptosis, i.e. programmed cell death (18). Biomaterials are usually designed to promote cell adhesion. However, they can also be designed to prevent it. It has been reported that nanotopography reduces adhesion of some cell types (e.g. fibroblasts) and improves adhesion of the others (e.g. muscle cells and astrocytes) (3). Cell type specific tendency for adhesion is possibly advantageous, since it can reduce the formation of redundant fibrous tissue and direct tissue growth around the implant (30).

Cell adhesion depends on the type and dimensions of the surface features. Thus, it has been shown that in early osteointegration of bone and dental implants regularly spaced pits or pillars on the surface of implant reduced, while grooves and steps improved cell adhesion (18). Khan *et al.* cultured neurons on nanostructured silicon. Nanofeatures with dimensions of 64 nm promoted adhesion, but both higher and lower material roughness reduced it (32). In another study Fan *et al*. grew neurons on silicon wafer surface. Neurons survived for more than 5 days on the surfaces with features 20 nm to 50 nm in size, while cell adhesion was adversely affected, when feature size was less than 10 nm or above 70 nm (33).

1.5.2. Effects of nanotopography on cell morphology and alignment

Gnavi *et al.* investigated Schwann cells from peripheral nervous system, which were grown on aligned gelatin fibers with diameter of 200–250 nm. They stretched in the same direction that the fibers were aligned; however, their adhesion and proliferation were reduced (34). Martínez *et al.* showed that cells seeded onto nanogrooves align their shape and elongate in the direction of the grooves. The study also demonstrates that degree of alignment is affected by cell type as well as by depth and width of the grooves (3).

If the depth of grooved microsurface features is increased and the width of the features decreased, this usually boosts cell alignment; however, this is not the case when the topography is nanostructured. Loesberg *et al.* cultured fibroblasts on linearly patterned surfaces and determined that groove feature depth below 35 nm or ridge feature width below 100 nm does not result in cell alignment. Also, in the case of fibroblasts, 35 nm feature size was the minimum depth for cell alignment (35). Teixeira *et al.* cultured human corneal epithelial cells on groove spacing ranging from 400 nm to 4000 nm. When groove spacing was bigger than 400 nm, cells started to align parallelly; however, when groove spacing was smaller than 400 nm, cells aligned perpendicularly. This indicates that for nanosurfaces there is minimal feature size limit that cells can still recognize, and below this limit cells do not respond to any additional changes in surface topography (36).

1.5.3. Effects of nanotopography on cell proliferation and differentiation

The effects of surface nanotopography on cell proliferation mostly depends on the cell type and type of surface features involved (3). Gerecht *et al.* showed that human embryonic stem cells react to substrate nanotopography with reduced proliferation (37). In another case human corneal epithelial cells were grown on polyurethane surfaces with ridged patterns 200-2000 nm in size. Feature sizes below 1 μm reduced cell proliferation (10). Cao *et al.* cultured astrocytes from rat nervous system on electrospun polymer fibers with average diameter of 665 nm. The cells exhibited reduced proliferation and increased apoptosis on the nanofiber surface compared to the growth on a flat surface of a polymer film (38).

Even though reduced proliferation is the most common cell response; some studies claim increased cell proliferation on nanostructured surfaces. Zhang and Webster observed breast adenocarcinoma cell and healthy breast cells on different PLGA nanosurfaces (flat, 23 nm, 300 nm and 400 nm). For cancer cells they observed significant decrease in proliferation

rate and vascular endothelial growth factor synthesis on surfaces with 23 nm features, while apoptosis was increased. At the same time proliferation of healthy cells on PLGA surface with 23 nm features increased. These findings indicate the possibility of using specifically designed polymer nanosurfaces as an alternative or a complementary approach to chemotherapy in anticancer regenerative medicine (39).

Popat *et al.* demonstrated increased ECM production of marrow stromal cells on nonporous alumina substrate surface (40). Dalby *et al.* showed that randomly distributed nanospheres on the surface direct and elevated mesenchymal stem cell differentiation (41). Kantawog *et al.* reported that human osteoprogenitor cells respond to nanopores and nanopits with increased differentiation and ECM production (42).

1.5.4. Influence of material characteristics on cell response *in vitro*

In vivo cells come in contact with various stimulants at the same time and this aspect should be considered in case of *in vitro* studies. Material properties, physical (surface topography, porosity), mechanical (elasticity, hardness) and chemical (functional groups, biological moieties, surface charge, surface energy, hydrophobicity), have an impact on cell behaviour (7). These material properties have either synergistic or antagonistic effects on cells, so it is relevant to explore their simultaneous effects on cell response, however this broad exploration presents a challenging experimental task (1).

1.6. Nanoscale surface patterning techniques

Surface patterning techniques include chemical and physical methods to create specific features on a surface of the material (1). The method to pattern a surface should be repeatable to assure consistent cell response, it should be able to pattern large surface areas in relatively short time (high-throughput) and give good resolution of nanoscale features, all within acceptable costs (24).

Several methods have been developed for preparation of biomaterials with nanofeatures controlled at both two-dimensional (2D) (Fig. 3) and three-dimensional (3D) (Fig. 4) nanoscale level. Depending on the starting material, they can be produced by "top-down" or "bottom-up" methods. The top-down methods use larger sized material and incorporate nanoscale features onto it. The bottom-up methods exploit interactions between particles to (self) organize and form ordered 2D or 3D structures. Later are more affordable and easier

to handle, with no waste or leftover of unused material, however, the successful spontaneous self-assembly can be a big challenge (43).

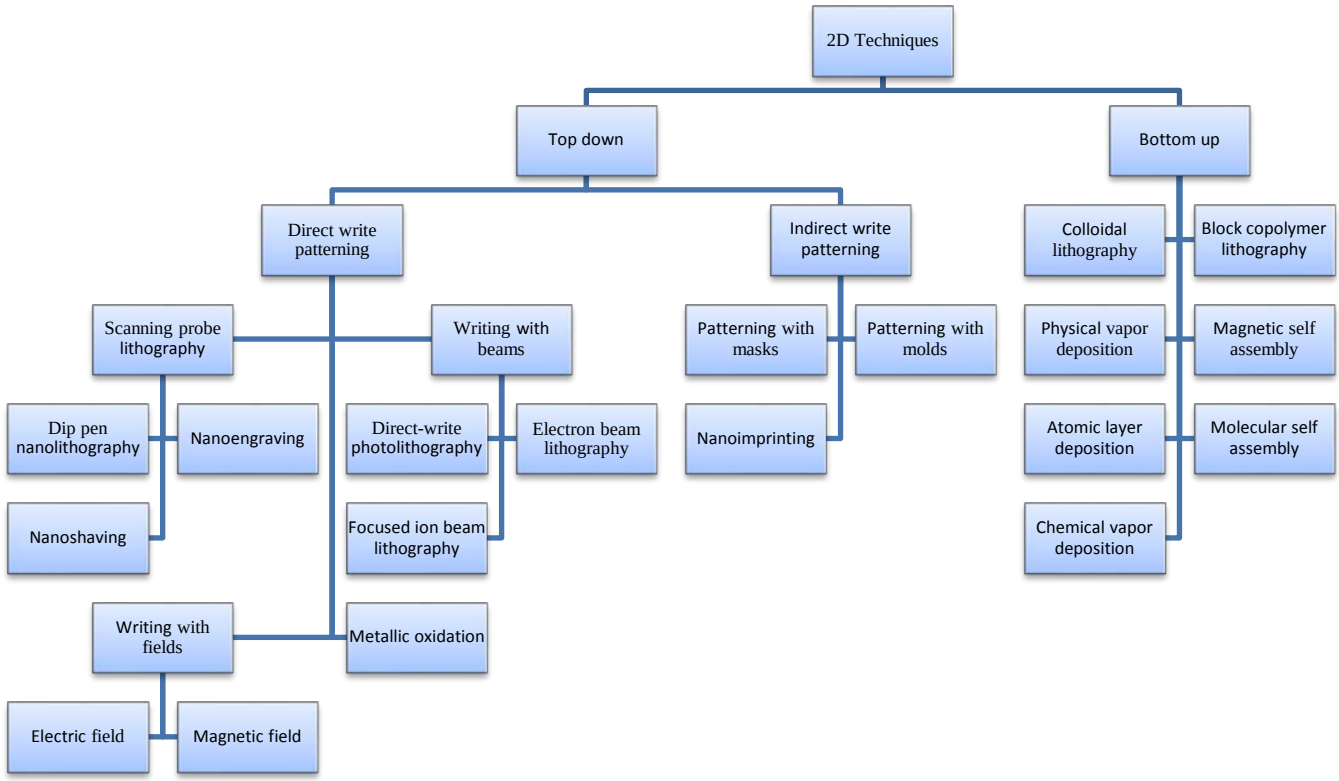

Fig. 3: Classification of 2D surface patterning techniques. Adapted from reference (1).

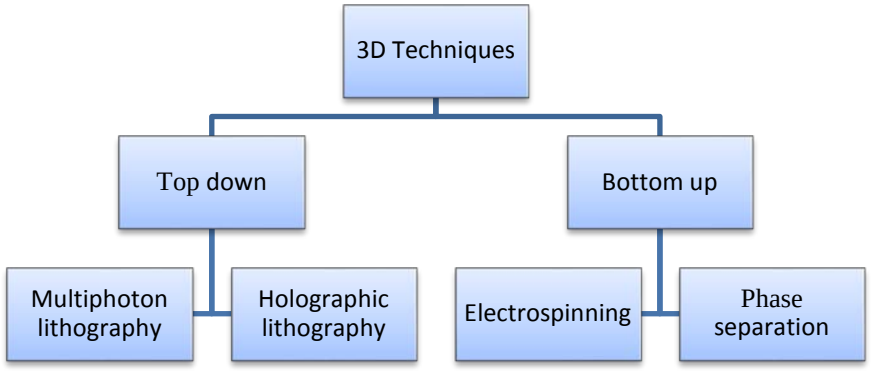

Fig. 4: Classification of 3D surface patterning techniques. Adapted from reference (1).

Different materials can be used to make nanotopographical models. Synthetic polymers, such as polypropylene (PP) (44), polycaprolactone (PCL) (45), poly-L-lactic acid (46), poly(acrylonitrile-co-methyl) acrylate (47, 48), and natural polymers (e.g. gelatin (34) and chitosan (49)) have already been used for fiber and filament production. PS (polystyrene) (50) and PLGA (51) have been used for grooved patterns. Polydimethylsiloxane (PDMS) (52, 53) and other silicones have been used for the development of substrates with grooves (54), pillars (55) and cones (56, 57). A thin layer of gold has been used for the fabrication of pores and pillars on a substrate (58). Substrates with random nanoroughness have been produced with the use of silica nanoparticles (59) or nanoporous gold surfaces (59, 60).

1.6.1. 2D Top-down direct-write patterning

Patterns of random high-resolution feature shape and size can be fabricated with direct-write patterning. These techniques are however low-throughput, slow and thus unsuitable for patterning over a large area (1).

1.6.1.1. Scanning probe lithography

In the process of scanning probe lithography (SPL) the molecules are deposited onto a surface in a certain pattern with a scanning probe. Near-field scanning optical microscopy (NSOM), scanning tunneling microscopy (STM) and atomic force microscopy (AFM) can be used to pattern the surface with nanofeatures (61).

Dip-pen nanolithography

In dip pen nanolithography (DPN), the tip of an AFM cantilever can be coated with proteins, peptides, DNA, small organic molecules, colloidal particles, polymers or metal ions. The tip then touches the surface and deposits the material in the predefined pattern. This technique is precise allowing the resolution below 50 nm, however, it is relatively low-throughput (18). If multiple probes are mounted on a scan head, high-throughput DPN can be carried out (1).

Engraving

Nanoscale engraving is a technique where a surface is mechanically cut or scraped with an AFM probe. The technique has similar advantages and disadvantages as DPN (1).

Nanoshaving

Nanoshaving can be applied when the deposited material on a surface needs to be removed. A layer of the surface is scratched away with an AFM tip, revealing the underlying material with a defined pattern (61).

1.6.1.2. Writing with beams

In these patterning methods an energetic beam is directed onto a surface to create a pattern. The spot size of the beam limits the resolution (1).

Direct-write photolithography

In direct-write photolithography a substrate is patterned directly by a beam of light. The resolution is limited by the wavelength of the light used, thus a minimum feature size is~200 nm (1). Novel approach with the use of deep ultraviolet light allows feature dimensions down to 50 nm (28). Direct-write photolithography is like engraving, the only difference is that the substrate material is instead of being physically scraped, deformed due to the high energy laser beam (1).

Electron beam lithography

The pattern is generated by a focused electron beam on the surface of material previously covered with electron-reactive material (61). The wavelength of electrons is shorter than the light, thus high-resolution features sizes 10-100 nm can be made (28). It is relatively expensive and requires high vacuum and dry samples. Furthermore, electron beam lithography is slow, thus only relatively small areas can be patterned (1).

Focused ion beam lithography

The pattern is generated by a focused ion beam. The ions collide with the atoms on the surface of material and etch them away. Focused ion beam lithography is similar to electron beam lithography in its advantages and limitations. High-resolution features sizes down to 20 nm can be made (3).

1.6.1.3. Patterning in electric or magnetic fields

Scanning electrodes enable occurrence of extremely localized electrochemical reactions, however writing in an electric or magnetic field is slow and thus not suitable to pattern large areas (1).

Patterning in electric field

An electrode is scanned near a surface, and patterns are created with charge or current. Local modification of the surface can be initiated through electrochemical processes, like charging, redox reactions and ohmic heating (1).

Patterning in magnetic field

Patterning in magnetic field is mainly used for storage of the data and not as a patterning method for biosurfaces. An inductive component is scanned above a material which is magnetizable, and the regions that are scanned become magnetized. These magnetized regions are used to store the data as bits (1).

1.6.1.4. Metallic oxidation

Oxidation of metallic substrate such as titanium can be applied to produce nanopits, nanotubes and nanopores on the surfaces. However, it is not easy to control the process and by now only the nanotubes were made without difficulties (28).

1.6.2. 2D Top-down indirect-write patterning

Patterning with application of masks - indirect-write photolithography

A mask is a template that masks specific regions of the substrate from the light exposure. Masks made from elastomeric polymers, like PDMS, fit non-flat surfaces and enable simple peel-off. Masks made from metal or metal and glass are rigid and easily cleaned (1). A photoresist is an organic material sensitive to light- used for coating of a substrate. It can be positive or negative. When a positive photoresist is exposed to light, the un-masked regions have higher solubility of photoresist in the developing solution and are removed by the developing solution. Sites with removed photoresist can then be etched away and after that the rest of the photoresist is removed, leaving behind a defined topography. When a negative photoresist is exposed to light, the areas that are not exposed are removed with the developing solution and exposed areas become cross-linked (61). Mask-based patterning is high-throughput technique by which complex features can be produced. The resolution of patterning with application of mask is ~ 200 nm (1).

Patterning with molds

When patterning with molds a soft polymer is used to create surface features on substrate in the process also known as *soft lithography*. A mold is a cast that is used to replicate patterns on the substrate. A mixture of monomer and curing agent is poured on a surface of the template and then cured. Upon separation, the cured polymer mold maintains the surface topography of the template. The pattern is later transferred to another material used for patterning. PDMS is most commonly used polymer in soft lithography, due to its elasticity and adherent nature. The method is relatively cheap and high throughput, but the resolution is not as high as with other indirect-write patterning techniques (1).

Nanoimprinting

Nanoimprinting is achieved by pressing together a mold, with the substrate under a certain pressure. Imprinting can be thermoplastic, photo- or electrochemical. In thermoplastic imprinting the pattern is transferred by pressure which causes subsequent heating of the polymer above its glass transition temperature and results in the pattern formation; in photo imprinting UV radiation generates the sufficient heat for patterning and in the case of electrochemical imprinting applied voltage generates heat for the formation of patterns. (61). In nanoimprinting features with dimensions below 25 nm can be formed over large surface area and the process is inexpensive (18).

1.6.2. 2D Bottom-up patterning techniques

Self assembly often occurs spontaneously in nature, e.g. the formation of the cell membrane lipid bilayers (61). The strategy behind bottom up patterning is the ability of atoms, molecules, colloidal particles and polymers to spontaneously self-assemble into defined architectures (18).

Atomic layer deposition

In the deposition of atomic layer, a material surface is exposed to the precursor, which then reacts with the surface. The reaction ends when all the reactive areas are occupied. The properties of the precursor-surface interaction thus control the thickness of the deposited layer, which is also the major advantage of atomic layer deposition technique (61, 62).

Molecular self assembly

In molecular self-assembly molecules assemble under equilibrium conditions with intermolecular or intramolecular forces into structurally stable aggregates, thus forming supramolecular systems (17). Common examples include self-assembly of surfactant molecules, resulting in formation of micelles, vesicles and liquid crystal phases. Nanostructures with diameters less than 20 nm can be created (61).

Colloidal lithography

In colloidal lithography interparticle forces tend to minimize the free energy of the system. That in turn causes separation and aggregation of particles in a specific pattern (1). Colloidal lithography is easy, repeatable and inexpensive way to make nanopatterns down to 50 nm (6).

Block copolymer lithography

Block copolymer in a solution is deposited onto a surface. The solvent evaporates and segregation of the microphase ends with formation of nanostructures over large surface area. Block copolymer lithography is affordable, simple and high-resolution method (18).

Physical vapor deposition

In physical vapor deposition (PVD) method, materials are first vaporized from a condensed phase and than recondensed on the surface of the substrate to form high purity metal, ceramic, semiconductor, insulator or polymer nanofilms. PVD is carried out in vacuum, which helps the vapors to reach the substrate and not interacting with other gaseous atoms (61).

Chemical vapor deposition

In chemical vapor deposition (CVD) hydrocarbons (methane, carbon monoxide, acetylene) in a gaseous state travel through the quartz tube heated to 720°C. The vaporized hydrocarbons are shattered due to the high temperature, producing pure carbon molecules, which bind to substrate, being heated and coated with a catalyst (Ni, Fe or Co) and thus a pattern is formed. Example of CVD in nanotechnology are carbon nanotubes with nanometre sized width (63).

Magnetic self assembly

In magnetic self assembly, magnetizable nanoparticles assemble in a magnetic field, due to their inherent dipole interactions and interparticle attraction (1).

1.6.3. 3D Top down patterning techniques

In vivo cells adhere to and react with 3D environment, which has been the main reason for 3D patterning techniques development. 3D patterns can be created through the combination of different 2D patterning techniques. For example, mask-based photolithography in combination with etching in multiple steps can build up 3D features (1). It is easier however, to use only one patterning technique.

There is a major interest in 3D printing in current research due to revolutionization of fabrication techniques, yet there is no proven technology that enables the production of the features in resolution needed for generation of nanotopography (64).

Multiphoton lithography

Multiphoton lithography or *direct laser lithography* is a multi-photon absorption process, where a laser scans a material that is transparent at the wavelength of the laser.

Photopolymerization takes place at the focal spot of the laser and can be regulated to create a three-dimensional pattern down to 100 nm feature dimensions (65). The 3D pattern becomes rigid and the remains of the uncured solution are rinsed away (1).

Holographic lithography

In holographic lithography a layer of photoresist is deposited on a substrate and four lasers are set in a way that they interfere with each other and create patterns in a resist. After the 3D shape has been created, the rest of the resist is washed away with developing solution (66).

1.6.4. 3D Bottom-up patterning techniques

Electrospinning

Electrospinning is the most common method for nanofiber production. They can be prepared from various synthetic and natural polymers like polylactic acid, PLGA, PCL, collagen, elastin, chitosan etc. (1). Under the influence of an electric field polymer solution forms a Taylor cone. The electrostatic forces form a fluid stream of the polymer solution, which travels towards the collector and starts to whip around quickly while the solvent evaporates, and fibers condense on the collector (67). The fiber diameter can be regulated by strength of electric field, molecular weight of the polymer, concentration and flow rate of polymer solution, and needle-collector distance (19).

Phase separation

In phase separation process the polymer is dissolved at high temperature in a solvent. The temperature is then decreased under the freezing point of the solvent, when the two phases separate. Solvent undergoes crystallization and can be removed through sublimation or freeze-drying (64).

1.7. Surface characterization of nanomaterials

To characterize surfaces after production scanning electron microscopy (SEM), STM and AFM are mainly used (1). Contact angle measurements and optical microscopy can also be a helpful tool for preliminary evaluation.

1.7.1. Contact angle measurements

By contact angle measurements surface wettability is measured directly, giving the information about surface hydrophilicity (1). An optimum value of surface hydrophilicity must be reached to enhance cell attachment since very hydrophilic or hydrophobic surfaces inhibit cell attachment (43).

1.7.2. Scanning electron microscopy

A high-resolution 2D image of the nanomaterial surface can be captured with scanning electron microscope (SEM). A high-energy electron beam is focused on a sample and interacts with the sample surface. Electrons with lower energy are emitted from the sample and their intensity is measured. SEM requires vacuum (1).

1.7.3. Scanning tunneling microscopy

In 1986 G. Binning and H. Rohrer won a Nobel prize for development of scanning tunneling microscopy, which was invented in 1881. A metal tip comes close (0.5-1 nm) to the sample surface that conducts electricity and an electron tunneling current is established. This current is monitored, and surface topography evaluated. STM works well for samples in aqueous environment, in air or under vacuum, if the sample is electrically conductive (1).

1.7.4. Atomic force microscopy

AFM measures surface structures with high resolution and accuracy. A great advantage over other imaging techniques (like SEM, STM) is that almost any surface of the sample can be imaged, from hard ones like ceramics to very soft ones, like polymers. Moreover, AFM can produce detailed 3D rather than 2D images without expensive and time-consuming sample preparation (68). There is no need for vacuum in AFM, so the imaging can be done in an air atmosphere or liquid conditions (69).

Unlike optical and electron microscope that form an image by focusing light or electrons to the sample surface, AFM "senses" the sample’s surface with a cantilever tip (Fig. 5).

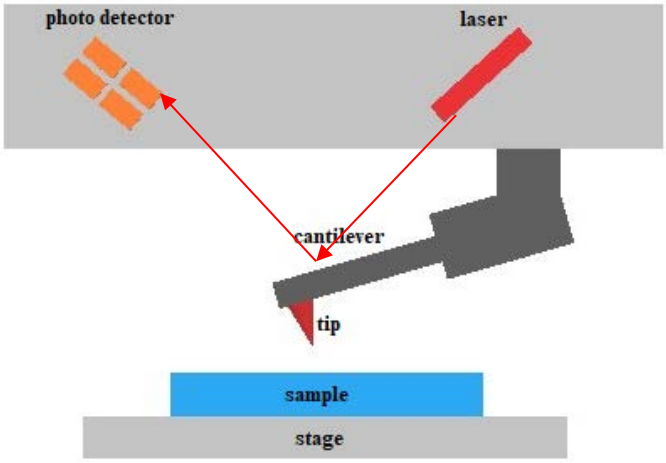

Fig. 5: Scheme of AFM. A sharp cantilever tip physically ‘feels’ the sample surface. The sample is mounted to the stage. A cantilever probe is displaced when it interacts with sample surface; consequently, the reflection of the laser beam is displaced on the surface of the photo detector. Adapted from reference (31).

The three basic components of AFM are piezoelectric scanner, transducer and feedback control. A sharp tip mounted at the end of cantilever moves over the surface of the sample. The transducer ‘feels’ the force between the surface and the tip, and the detector receives a signal and then sends it back to the scanner, which keeps a steady distance between sample surface and the tip (68).

There are some limitations of AFM. The depth of the field of view is limited by the travel distance of piezoelectric scanner, its tip size and geometry (69).

2. OBJECTIVES

The goal of our research is to develop novel nanostructured films from biodegradable polymer, namely PCL. The surface of the films will mimic the nanotopography of ECM and therefore it is expected to have an influence on cell behavior, primarily on cell adhesion. The potential applicability of such films with nanostructured surfaces is in various areas including pharmaceutical sciences, biomedical and tissue engineering. They can be used for various purposes including drug delivery, delivery of biomacromolecules and in tissue regeneration. Once such films are administered in the body, they will degrade after a certain time, without causing any side effects.

To produce nanosized features on the surface of the films, an innovative method will be used, which combines colloidal lithography, nanosphere soft lithography method and polymer casting.

To create a negative relief in polydimethylsiloxane (PDMS), polystyrene (PS) templates will be prepared by using five different aqueous suspensions of PS nanobeads with average size of 27 nm, 62 nm, 99 nm, 210 nm and 280 nm. Positive relief of PS template nanosurface will then be made by pouring solution of PCL in chloroform onto the PDMS molds. The topography of produced films will be evaluated by AFM imaging, the uniformity of the ordered nanosurface will also be evaluated.

3. MATERIALS AND DEVICES

3.1. Materials

- Silicon wafers (Sigma-Aldrich, USA)

  A silicon wafer is a thin, flat slice of semiconductor material, which mainly serves as a substrate for microelectronic devices. Wafers are formed of highly pure, nearly defect-free single silicon crystalline material (70).
- Milli-Q water (resistivity 18.2 MΩ cm^{-1} at 25 °C) (Merck Millipore, USA)
- PS nanobead aqueous suspensions 10% (w/w) with beads in diameters of 27 nm, 62 nm, 99 nm, 210 nm and 280 nm (Bangs Laboratories, Inc., USA)
- PDMS Sylgard 184 silicone elastomer base and curing agent (Dow Corning, USA)
- PCL average M_n 45,000 (Sigma Aldrich, USA)

  PCL is biodegradable polymer that is semi-rigid at room temperature. It degrades at a slowly rate and can therefore be used in drug delivery devices that degrade for over a year. PCL is regarded as nontoxic and tissue-compatible material (1).
- Sodium dodecyl sulfate (Merck KGaA, Germany)

3.2. Equipment

- Borosilicate glass Petri dish (Isolab, Germany)
- Aluminum foil (İlsan Pharmaceuticals, Turkey)
- TPP Multiwell Tissue Culture Plate, 24 well cell culture plate (Midsci, USA)
- Micropipettes (Rainin, USA)
- BD Precisionglide® syringe needles 26G (Sigma Aldrich, USA)

3.3. Devices

- VWR® Ultrasonic cleaner (VWR International, USA)
- MS2 Minishaker (IKA-Works, Germany)
- UV/Ozone ProCleaner™ Plus (BioForce Nanosciences, Inc., USA)
- Ambient AFM™ (Nanomagnetics Instruments, UK)
- PPP-NCLR AFM probes nominal resonance frequency: 190 kHz, nominal force constant: 48 N/m (Nanosensors, Switzerland)

- NMI Image Analyzer v1.5 (Nanomagnetics Instruments, UK)
- Optical microscope (Olympus SZX7, Japan) equipped with a digital camera (Olympus C-5060, Japan).
- Aseptic laminar flow hood (Thermo Fisher Scientific, USA)
- Vacuum oven OV-02 (Medline Scientific, UK)
- Ecocell oven (MMM Group, Germany)
- Balance (Mettler Toledo, USA)
- Magnetic stirrer Rh basic (IKA, Germany)

4. METHODS AND PROCEDURES

4.1. PS template sample preparation

Silicon wafers were used as a base for PS templates. PS templates were prepared as reported previously (71). Briefly, silicon wafers were cut in square sized pieces (1.5 x 1.5 cm^2). To cut the silicon wafers, a spatula was used instead of a knife, since the wafers are easily chipped and scratched. The wafer cuts were then cleaned with VWR® Ultrasonic cleaner and UV/Ozone ProCleaner™ Plus. Wafer cuts were put into a beaker filled with ethanol, which was then placed in the ultrasonic bath (VWR® Ultrasonic bath) and sonicated in ethanol for 10 min. The cuts were then washed with Milli-Q water, dried and put in the UV/Ozone ProCleaner™ Plus for 20 min (Fig. 6).

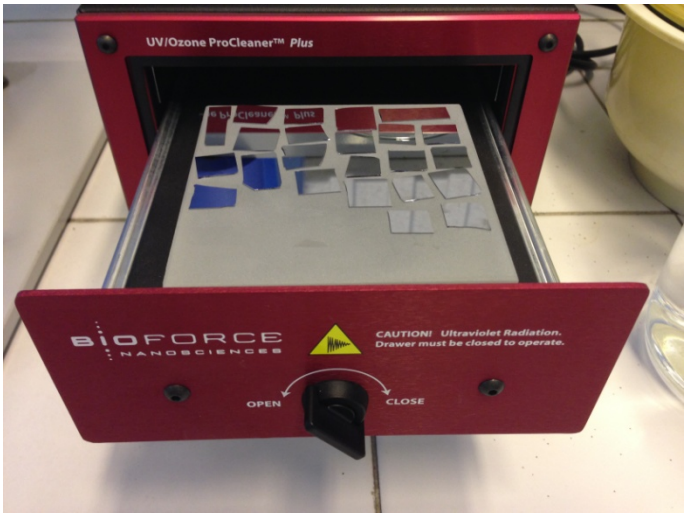

Fig. 6: Incubating silicon wafer cuts in UV/Ozone ProCleaner™ Plus to increase hydrophilicity of the wafer surface.

A clean silicon surface is hydrophilic, i.e. it is completely wetted by water The Petri dish was filled by half with Milli-Q water and a piece of silicon wafer was then leaned on the edge of the Petri dish at an angle of ~120°, serving as a slide to the water surface (Fig. 7 a).

a)

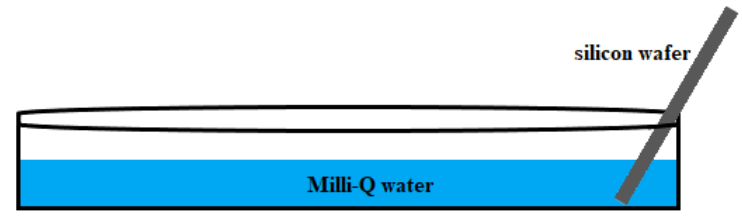

b)

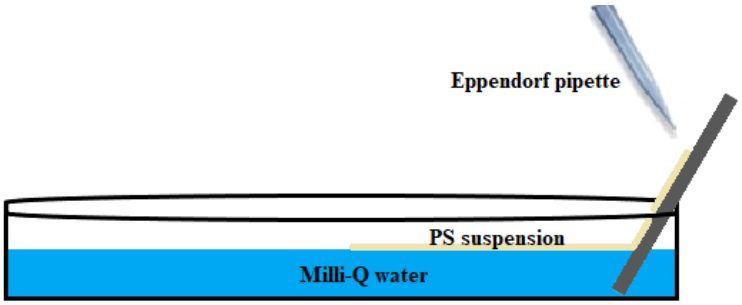

Fig. 7: PS template sample preparation. a) The Petri dish is filled with Milli-Q water and silicon wafer piece leaned on the edge, b) PS suspension is slowly put on the water surface with an Eppendorf pipette.

PS nanobead suspension (100 µL, 10 wt.%) was mixed with an equal amount of ethanol, using MS2 Minishaker. This mixture was slowly added through inclined wafer piece onto the water surface using an Eppendorf pipette (Fig. 7b). The process was repeated with PS nanobead suspensions of 27 nm, 62 nm, 99 nm, 210 nm and 280 nm in diameter. To obtain close packed formation of the particles on the water surface, the solution of 2% sodium dodecyl sulfate (~10 µL SDS, Merck) was added. The detergent molecules decrease surface tension of water and push the nanobeads on water surface close together. Silicon wafer cut was then slowly submerged in the water with a spatula, picking up a monolayer of PS nanobeads on the water surface. Wafer cuts were then dried at room condition so dry. Some silicon wafer cuts were left untreated and served as a reference material to prepare non-textured films, which were used as a control.

4.2. PDMS mold sample preparation

PDMS molds were prepared as reported previously (71). Briefly, aluminum foil was put on the bottom of a Petri dish. Six PS template silicon wafer cuts (1.5 cm x 1.5 cm) covered with same sized nanobeads were put on aluminium foil with the nanobeads treated surface facing up. PDMS was mixed thoroughly in a Falcon centrifuge tube according with the manufacturer's instructions (curing agent: base, 1: 10 (w/w)) and then poured over PS template silicon wafer cuts. Petri dishes were then placed in a vacuum oven over the night. Afterwards they were put into an Ecocell oven at 40°C for 2 h. After curing for 24 h, aluminum foil and all six PS template wafer cuts were carefully removed from PDMS mold (Fig. 8).

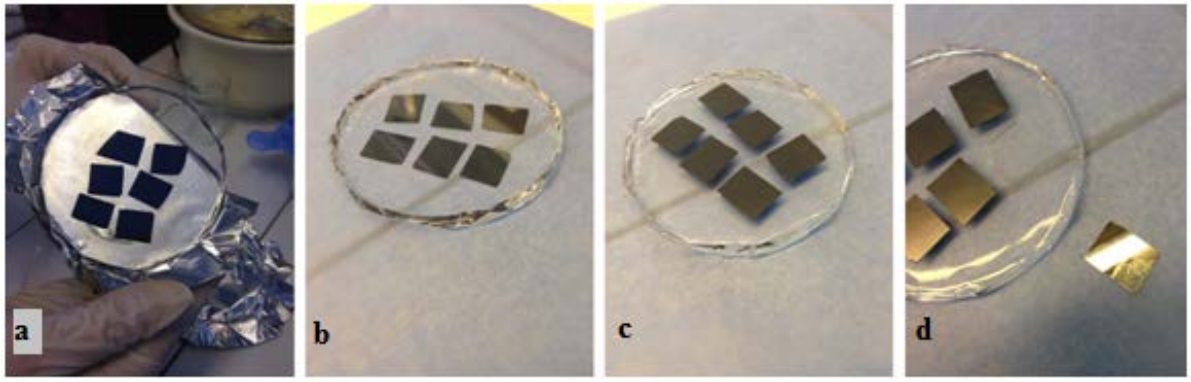

Fig. 8: Preparation of PDMS molds. a) Removal of aluminum foil from the bottom of the mold after curing, b) PDMS mold with PS templates on the bottom of the mold with nanostructured surface facing up, c) inverted PDMS mold, PS templates adhering to the top of the mold with surfaces facing down, d) careful removal of the silicon wafer cuts from the surface of inverted PDMS mold, leaving the negative relief of PS template topography in the mold.

Finished PDMS mold was washed with acetone. For each nanostructured PS template (27 nm, 62 nm, 99 nm, 210 nm and 280 nm) 3 parallel PDMS molds were prepared. Blank molds were prepared by using untreated i.e. smooth silicon wafer pieces.

4.3. PCL film sample preparation

Polymer films were prepared from PCL. Developed PDMS molds were placed in Petri dishes. 10% (w/V) solution of PCL in chloroform was poured over each section of PDMS mold (1.5 cm x 1.5 cm). The Petri dishes were then placed in a vacuum desiccator. After 48 h, when solvent evaporated, PCL films were carefully peeled off the molds. PCL films with feature sizes of 99 nm, 210 nm and 280 nm, as well as control films were prepared. Since it is not possible to distinguish with a naked eye which side of the film has nanostructured surface, the non-nanostructured side was marked using a marker.

4.4. AFM imaging

Topography of PS templates, PDMS molds and PCL films was analysed in air by AFM (Ambient AFM^{TM}, Nanomagnetics Instruments) operating in dynamic mode, with an E-scanner at scan rates between 0.5–1.5 Hz. PPP-NCLR AFM probes were used for image acquisition. Samples of PS templates, PDMS molds and PCL films were glued onto a metal plate, which was later fixed to an AFM magnet (Figs. 9 and 10).

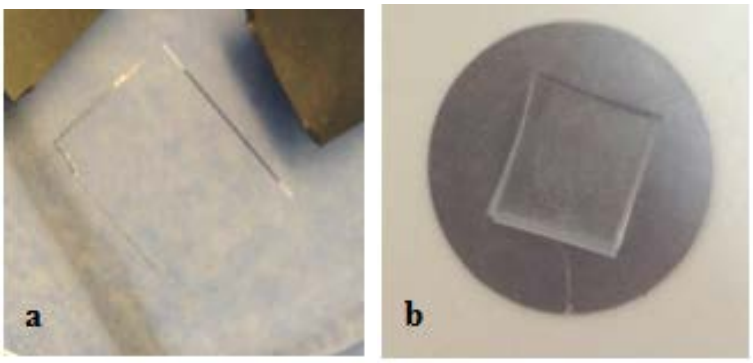

Fig. 9: AFM sample preparation. PDMS mold sample fixation to a metal plate. a) Close-up image of PDMS mold sample in silicon, b) image of PDMS mold sample cut-out glued onto a metal plate.

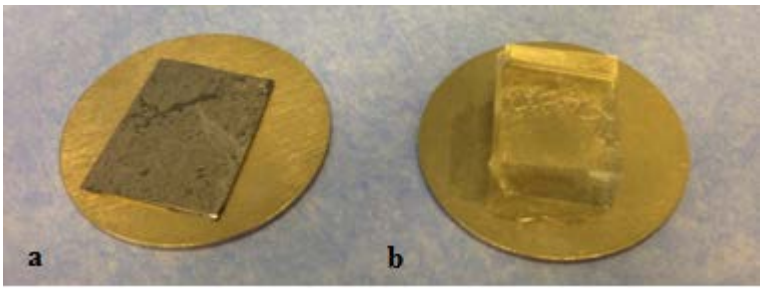

Fig. 10: AFM sample preparation. a) PS template fixed onto a metal plate, b) PDMS mold sample fixed onto a metal plate.

It took considerable amount of time for successfully AFM imaging. After the AFM was turned on it needed around 45 min for the piezoelectric scanner to reach its balance. Then, the parameters adjustment took place, before first measurements were done. Each measurement lasted for around 40 min. Since the images can easily get disrupted by sounds or vibrations, sometimes the measurements needed to be restarted. To perform all measurements for each size of nanotopography it took at least one week of measurements. Imaging of samples with diameters of 27 nm and 62 nm sized nanotopography took longer due to repeated imaging, to make sure that no regular topography can be observed.
Images of PS template samples, PDMS mold samples and PCL film samples, prepared with PS nanospheres with size of 27 nm, 62 nm, 99 nm, 210 nm and 280 nm, as well as control samples were recorded.

4.5. Preparation of samples for the study of cell response to nanostructured surfaces

For investigation of cell response to nanostructured surfaces a method was used described in publication for sample preparation for the cell culture on plasma-coated electrospun scaffolds (72). PDMS silicone (curing agent: base, 1:10 ratio (w/w)) was prepared and poured on the bottom of 24 well cell culture plate with a plastic syringe to serve as a scaffold after being cured inside of wells. Wells were one-third filled with PDMS and left to dry for 48 h (Fig. 11). PCL films were cut in a round shape fitting a well (Fig. 12) and placed on the dried silicone with nanostructured surface facing up.

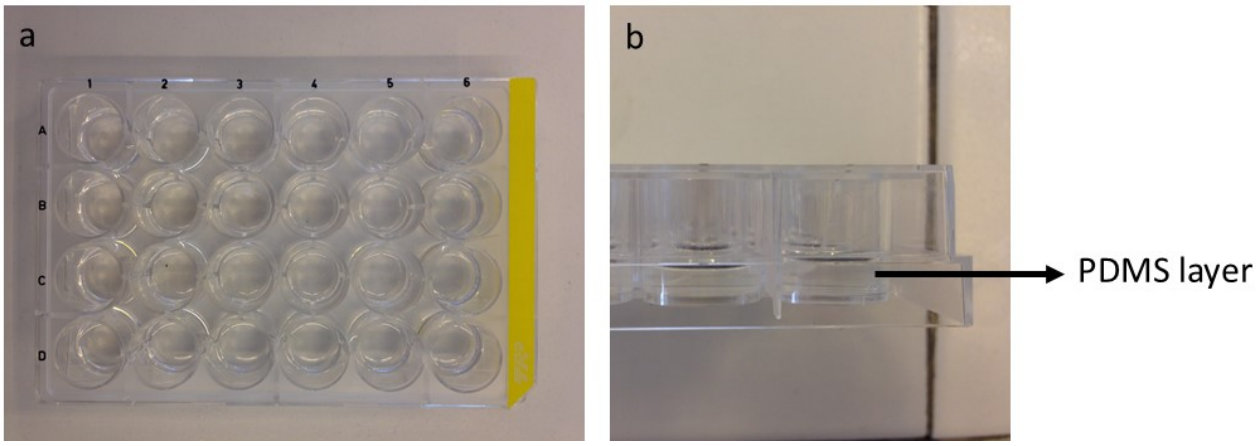

Fig. 11: Preparation of PDMS covered wells for preliminary study of cell response to nanostructured topography on (human ovarian cancer) cells (OVCAR3); top view (a) and side view (b).

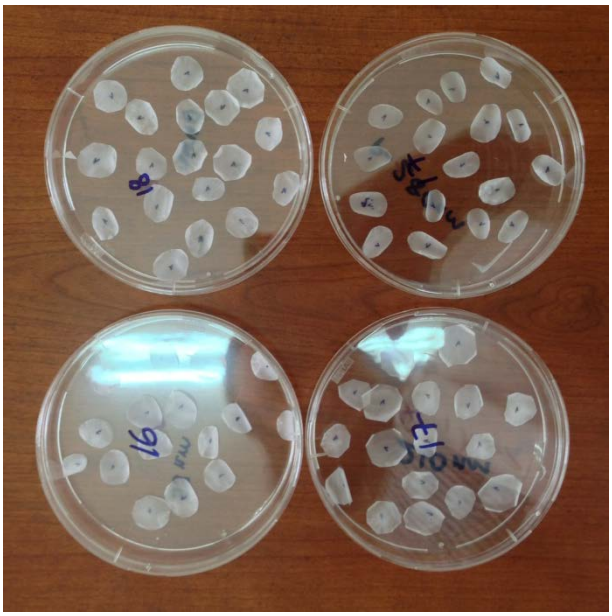

Fig. 12: PCL film samples of 99 nm, 210 nm and 280 nm surface feature dimensions and smooth PCL film samples in Petri dishes prepared for cell culture experiments. Films were cut in round shape and marked on non-nanostructured side.

Each film was fixed in the middle of well with a thin BD Precisionglide® syringe needle pierced through the film into the PDMS base (Fig. 13).

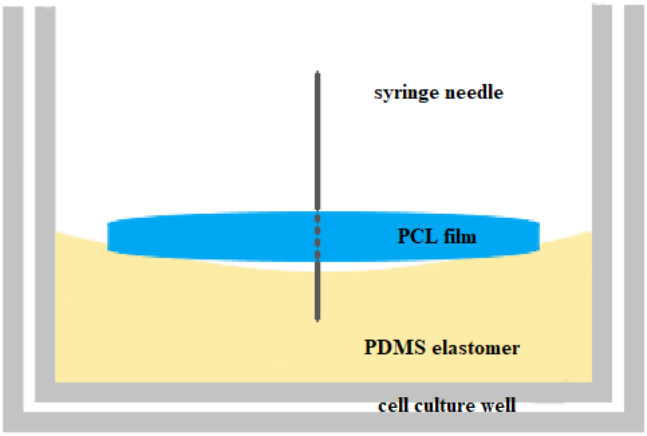

Fig. 13: Schematic illustration of the setup of the PCL film in a well with nanostructured surface facing up. Cut syringe needle is used to fix the film in the middle of the well. Adapted from reference (72).

The bottom of the needles (plastic end) was cut by pliers so the well plates could close without difficulties. Four 24 well cell culture plates were used, each for different nanostructured PCL films (control, 99 nm, 210 nm and 280 nm). 15 wells of each culture plate were filled with nanostructured PCL films. The rest were left empty as control). Cell culture plates with nanostructured films were then surface sterilized under UV light for five hours.

5. RESULTS AND DISCUSSION

Our aim was to develop a method, which would enable fabrication of uniform and defect-free nanostructured surfaces on biodegradable PCL films, with high resolution over surface area (1.5 cm x 1.5 cm) needed for the with the cell culture experiments.

The method of Rybczynsky *et al.* was used for PS template preparation (73). Silicon wafer were cleaned with UV/Ozone ProCleaner™ Plus by a high-power UV light source. UV light generates ozone, which disintegrates contaminants on the surface, making them volatile. Volatile compounds evaporate and leave the surface clean and more hydrophilic (74). Increased hydrophilicity was important to transfer the layer of PS nanobeads on the water surface on the silicon wafer evenly in one layer. PS templates were prepared by the method of self assembly of PS nanospheres on water surface which were transferred on a wafer in a single layer. PDMS templates were then developed through molding process i.e. soft lithography and nanopatterns transferred on PCL films by casting of PCL solution in chloroform in the PDMS mold. After evaporation of chloroform, a thin rigid PCL film with nanostructured surface was prepared (Fig. 14).

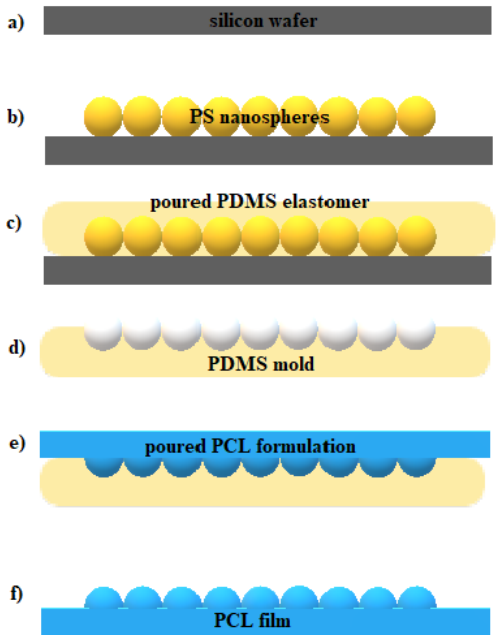

Fig. 14: The process of PCL film sample development with help of PS template and PDMS mold: a) silicon wafer cut - lateral view, b) PS nanospheres covering silicon wafer cut in a monolayer, c) PDMS elastomer poured on PS template, d) PDMS mold removed, turned and placed back in the Petri dish, e) PCL solution poured on inverted PDMS mold, f) uniform nanostructured surface of PCL film.

This method was developed by Yaşayan *et al.*, where PLGA was used to create nanostructured biodegradable films for investigations of human ovarian cancer cell attachment (71).

5.1. PS template and PDMS mold sample preparation

The surface of PS templates should be completely dry before putting them in the Petri dish and pouring over the PDMS, otherwise holes are made in the PDMS mold upon separation of templates from the mold. Aluminum foil was placed on the bottom of Petri dish, not to contaminate it with silicone and to enable easy removal of PDMS molds after being cured. Aluminum foil should not be damaged in this process, since then it is impossible to remove wafer pieces. The rigidity of the mold is controlled by curing agent: monomer ratio and the incubation time of preparation. When the PDMS mold is cured it keeps the shape with high accuracy of the features implemented (25).

Silicone was poured onto the wafers in a Petri dish slowly and then left in a vacuum oven over the night to remove residual air bubbles. To accelerate curing wafers were heated to 40°C for at least 2 h. Finished PDMS molds of 27 nm, 62 nm, 99 nm, 210 nm and 280 nm sized features and control PDMS molds were submerged into acetone to remove PS beads remaining and other possible contaminants.

5.2. PCL film preparation

The PCL polymer was chosen for the study based on its slow biodegradability over a period of time and at the same time enabling a prolonged release of the active ingredient. A good example is a study by Bolgen *et al.*, where PCL membranes, used for treatment of abdominal adhesions in animal after surgery, were loaded with antibiotic. In a 3 h period, 80% of the antibiotic was released from the membrane, and the rest in the next 18 h. Degradation time of the PCL membrane was significantly longer. Compared to control the membrane effectively restrained adhesions and improved healing (75).

PCL films were prepared in an aseptic laminar flow hood not to contaminate the samples and to avoid chloroform vapor inhalation. When PCL solution in chloroform was poured in the PDMS mold, the mold swelled, and the PCL solution flew over the edges of the template (Fig. 15). To prevent the swelling of the PDMS mold, double sided tape was used to tape and fix it to the bottom of the Petri dish.

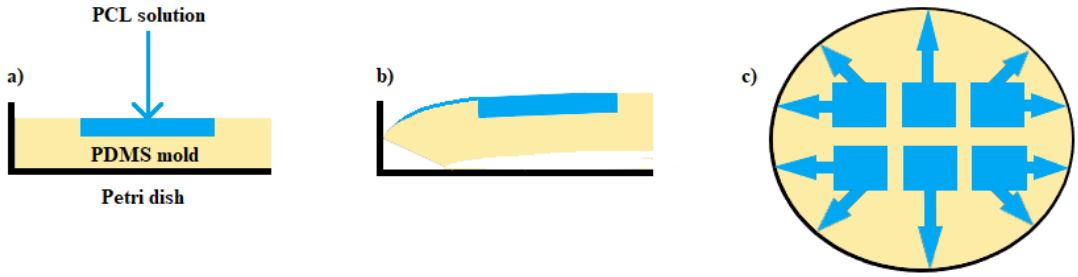

Fig. 15: a) Petri dish side view: PCL solution poured in the PDMS mold, b) swollen PDMS mold with PCL solution flowing over the edges of PDMS mold, c) Petri dish top-view: PCL solution flowing over the edges of PDMS mold in different directions.

Another solvent, namely dichloromethane was tested for preparation of PCL films to prevent mold swelling and leaking. By using dichloromethane PCL solution, the PDMS mold did not swell so much, however the quick evaporation caused entrapment of many residual air bubbles within the PCL film. The air bubbles disrupted the surface of the film, so we continued the experiments with PCL chloroform solution which enabled the formation of even rigid films.

5.3. AFM sample characterization

The samples were prepared as described in section *Methods and procedures*. Images of PS template samples, PDMS mold samples and PCL film samples as well as control samples were recorded (Figs. 16 and 17).

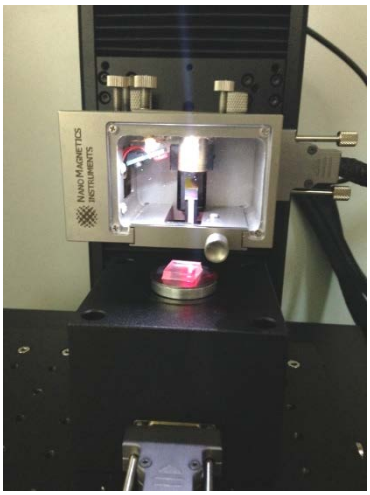

Fig. 16: AFM scanning of PDMS mold sample with Ambient AFM™ operating in dynamic mode, with an E-scanner at scan speed of 0.5–1.5 Hz.

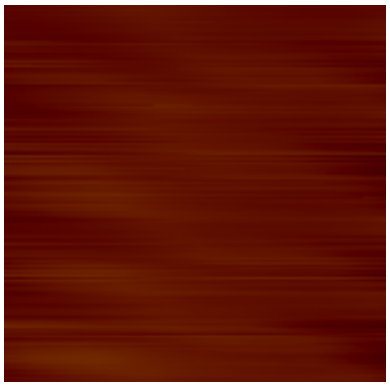

Fig. 17: AFM image of the topography of control PCL film surface. The image represents the scan of surface area 2 µm x 2 µm.

PS templates with feature diameters of 27 nm and 62 nm did not prove to be effective. Nanobeads seemed to be too small and thus created multilayers on the surface of the silicon wafer (Fig. 18), which resulted in more disturbed topography observed on AFM images and unsuccessful PS template and PDMS mold fabrication (Fig. 19, 20, 21, 22). PCL films with 27 nm and 62 nm topographies were therefore not produced.

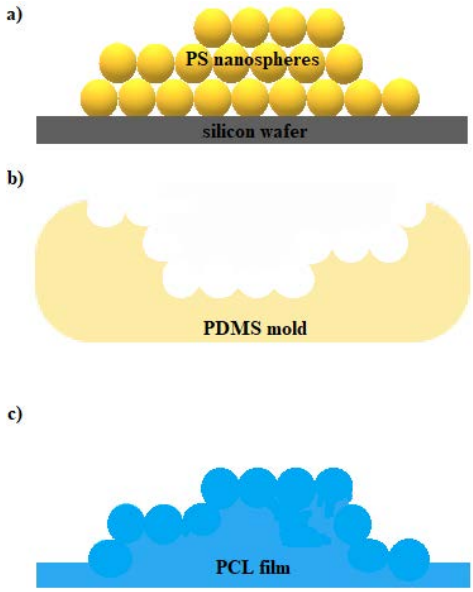

Fig. 18: Irregularity in PCL film due to the multilayering effect in the initial step of PS template preparation: a) PS nanobeads covering silicon wafer cut stacking on top of each other, b) irregular PS template surface transferred to PDMS mold, e) non-uniform, uneven surface topography of PCL film.

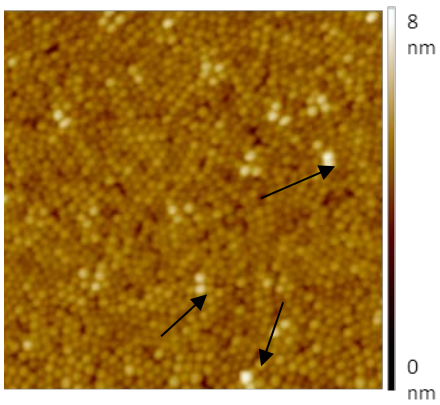

Fig. 19: AFM image of 27 nm nanostructured PS template surface. PS nanobeads were successfully transferred to the silicon wafer, however there were areas of multilayers of the PS beads on the template. The arrows indicate brighter areas, representing multilayers of PS nanobeads. The image represents the scan of 2 µm x 2 µm surface area.

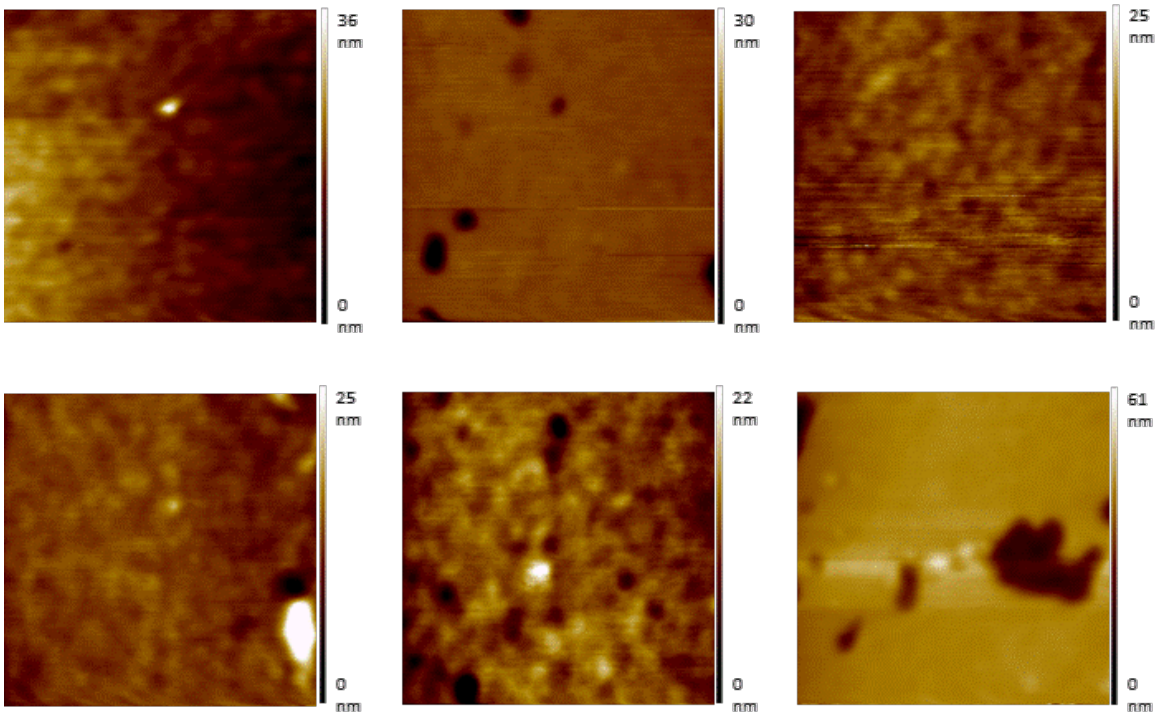

Fig. 20: AFM images of six different PDMS mold samples created by PS templates with 27 nm nanostructured surface. The surfaces did not exhibit regular topography of 27 nm. The topography of PS templates was not transferred to any sample of the PDMS molds. The samples are similar to PDMS control sample. The image represents the scan of surface area 2 µm x 2 µm.

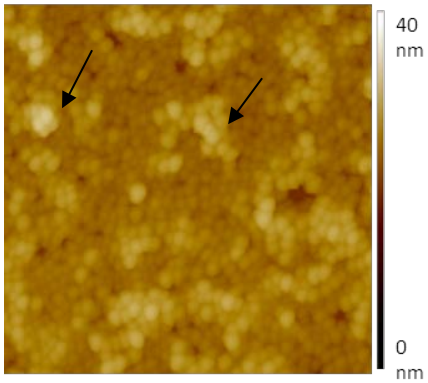

Fig. 21: AFM image of 62 nm nanostructured PS template surface. PS nanobeads were successfully transferred to the silicon wafer, however similar to the 27 nm nanostructured PS template surface, there were areas of multilayers of the PS beads on the template. The arrows indicate brighter areas of multilayering of PS nanobeads. The image represents the scan of surface area 2 µm x 2 µm.

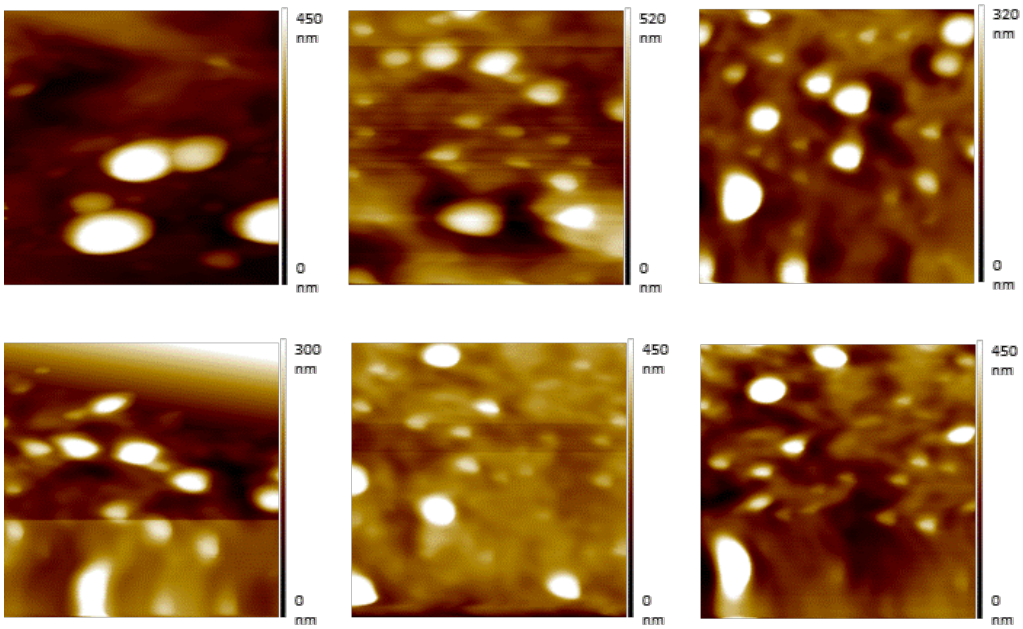

Fig. 22: AFM images of six different PDMS mold samples created by PS templates with 62 nm nanostructured surface. The surfaces did not exhibit regular topography of 62 nm. The topography of PS templates was not transferred to any sample of the PDMS molds. However, compared to PDMS mold samples of 27 nm, there are brighter areas that indicate that some kind of topography was transferred. The image represents the scan of surface area 2 µm x 2 µm.

The smallest diameter of the PS nanospheres which can organize in a monolayer was 99 nm. This can be seen in AFM images which show an even arrangement of the features on PS templates, however brighter multilayered areas and darker disrupted areas were still observed on the surface which projected in the PDMS mold and later the PCL film (Fig. 23).

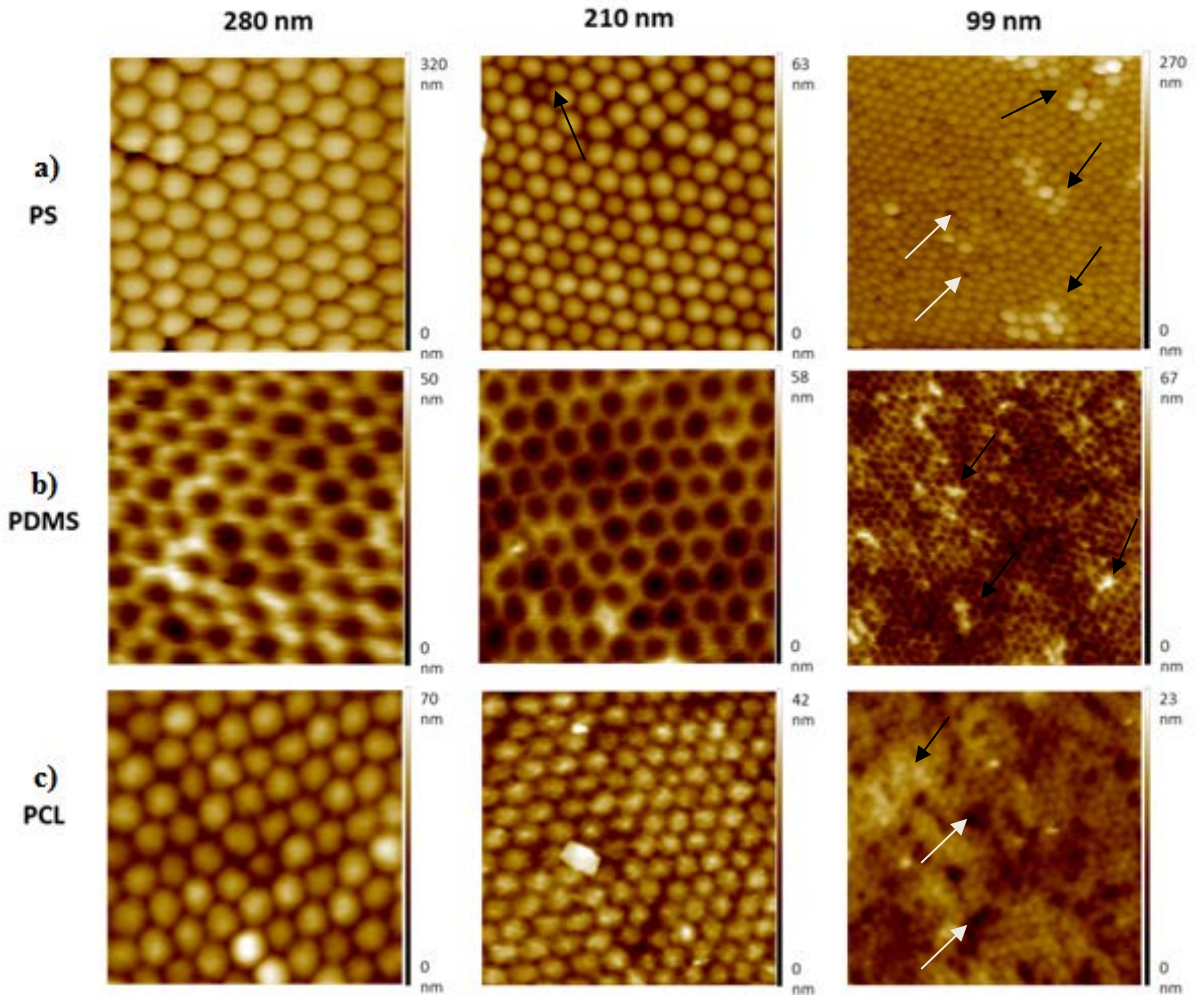

Fig. 23: AFM images of PS template samples (a), PDMS mold samples (b) and PCL film samples (c) prepared with nanospheres with diameter of 99 nm, 210 nm and 280 nm. Multilayered areas indicated with black arrows, disrupted areas indicated with white arrows. The image represents the scan of 2 µm x 2 µm surface area.

AFM images of 210 nm and 280 nm feature diameters showed that PS monolayered templates were well prepared, however there are some disrupted areas in the case of 210 nm surface where a single PS bead is missing. Features were then transferred to PDMS mold and PCL film with highly ordered defect free hexagonal packing (Fig. 23).

In a study by Yaşayan *et al.* nanostructured PDMS and PLGA surfaces with feature dimensions of 57 nm, 99 nm, 210 nm and 280 nm were prepared from monolayered PS templates. 57 nm PS templates did not produce a clear topography. We were also not able to create PS templates with 27 nm and 62 nm feature topography. We can assume that the smallest feature dimension for successfully preparation of a hexagonal topography on silicon wafer with this method is about 99 nm.

On AFM images of PDMS and PLGA surfaces prepared by Yaşayan *et al.* from monolayer PS templates, multi-layers were observed with 99 nm surface features. In our study we obtained similar results with PDMS and PCL surfaces. However, the images of that study showed highly disrupted surface regularity, whereas in our images the surface observed was less disrupted and hexagonal shape was more clearly seen.

The surfaces formed by 210 nm and 280 nm features prepared by Yaşayan *et al.* on PDMS and PLGA surfaces formed clear structures and the same clarity was observed in our case with same size features on PDMS and PCL surfaces.

5.4. Preliminary studies of cell response to nanostructured PCL films

MTT assay was carried out by Associate Professor Oya Orun and Associate Professor Pınar Mega Tiber at external institute (Marmara University, School of Medicine, Department of Biophysics). The syringe needle used for film fixation made the film dimpled within the cell culture medium during the assay. Unfortunately, it was thus not possible to capture images of OVCAR3 cell attachment, since the films were not flat. Even if the cells adhered to the films, it was impossible to prove it, since with curved films the surface topography would not be the only parameter to modulate cell behaviour. We can conclude that in order to test the cellular response to nanostructured films, a method for the proper preparation of films should be developed to prevent the dimpling of films in contact with the medium.

6. CONCLUSIONS

In this research we aimed to develop nanostructured PCL films. Surface topography was transferred from monolayered PS templates to PCL films through PDMS molds. Suspensions of PS nanobeads with diameters of 27 nm, 62 nm, 99 nm, 210 nm and 280 nm were used. Smooth silicon wafer served as a control. PS templates, PDMS molds and PCL films were characterized by AFM. Preliminary cell studies were carried out with PCL films using 24 well cell culture plates.

According to our results, we can conclude that

- With the method used 27 nm and 62 nm nanostructured surfaces cannot be created, due to multilayer PS nanobead formation resulting in uneven template topography.

- With this method nanostructured surfaces can be created with features of 99 nm or larger; however, some multilayered parts can also be formed, resulting in local surface homogeneity disruption.

- With this method defect free nanostructured surfaces can be created with features of 210 nm and 280 nm in diameter, which enables preparation of nanostructured films in this size range.

- Diameter of PS particles and concentration of SDS solution are important parameters in fabrication process. If particle diameter is smaller than 99 nm and concentration of SDS solution is too high, multilayered nanoparticle structures are formed.

- Comparable results, observed with a similar method used to make nanostructured PLGA films, show that the method can be used for nanostructuring of various polymer materials.

- Other solvents besides chloroform and dichloromethane should be tested to prevent PDMS mold from swelling and bubble formation within the PCL films and thus enable formation of uniform films.

- Different method for preparation of PCL film samples for cell study should be used to prevent the curling of the films in the cell culture medium and thus enable evaluation of the cell response to nanotopography.

7. LITERATURE

1. Ratner B D, Hoffman A S, Schoen F J, Lemons J E: Biomaterials science: An introduction to materials in medicine 3rd Edition, Academic Press, California, 2012: 276-1069.

2. Curtis A, Wilkinson C: Topographical control of cells, Biomaterials 1997; 18: 1573-1583.

3. Martínez E, Engel E, Planell J A, Samitier J: Effects of artificial micro- and nano-structured surfaces on cell behavior, Annals of Anatomy 2009; 191: 126-135.

4. Dalby M J, Riehle M O, Johnstone H J, Affrossman S, Curtis A S: Polymer-demixed nanotopography: control of fibroblast spreading and proliferation, Tissue Engineering 2002; 8(6): 1099-1108.

5. Miller D C, Thapa A, Haberstroh K M: Endothelial and vascular smooth muscle cell function on poly (lactic-co-glycolic acid) with nanostructured surface features, Biomaterials 2004; 25; 53-61.

6. Koegler P, Clayton A, Thissen H, Santos G N C, Kingshott P: The influence of nanostructured materials on biointerfacial interactions, Advanced Drug Delivery Reviews, 2012; 64(15): 1820-1839.

7. Skoog S A, Kumar G, Narayan R J, Goering P L: Biological responses to immobilized microscale and nanoscale surface topographies, Pharmacology & Therapeutics, 2017.

8. Harrison R: The reaction of embryonic cells to solid structures, Journal of Experimental Zoology Part A: Ecological Genetics and Physiology, 1914; 17(4): 521-544.

9. Weiss P: Experiments on cell and axon orientation in vitro: the role of colloidal exudates in tissue organization, Journal of Experimental Zoology Part A: Ecological Genetics and Physiology, 1945; 100(3): 353-386.

10. Brennan A B, Kirschner C M: Bio-inspired materials for biomedical engineering, Wiley & Sons Inc., New Jersey, 2014: 77-95.

11. Curtis A S G, Varde M: Control of cell behavior: topological factors, Journal of the National Cancer Institute, 1964; 33(1): 15-26.

12. Jenkins D H, Forster I W, McKibbin B, Ralis Z A: Induction of tendon and ligament formation by carbon implants, Bone & Joint Journal, 1977; 59(1): 53-57.

13. Kleinfeld D, Kahler K H, Hockberger P E: Controlled outgrowth of dissociated neurons on patterned substrates, Journal of Neuroscience, 1988; 8(11): 4098-4120.

14. Formhals A: Apparatus for producing artificial filaments from material such as cellulose acetate, Schreiber-Gastell, Richard, 1934; U.S.A. Patent.

15. Stitzel J D, Pawlowski K J, Wnek G E, Simpson D G, Bowlin G L: Arterial smooth muscle cell proliferation on a novel biomimicking, biodegradable vascular graft scaffold, Journal of Biomaterials Applications, 2001; 16(1): 22-33.

16. Xia Y, Whitesides G M: Soft lithography, Annual Review of Materials Science, 1998; 28(1): 153-184.

17. Donnelly H, Dalby M J, Salmeron-Sanchez M, Sweeten P E: Current approaches for modulation of the nanoscale interface in the regulation of cell behavior, Nanomedicine: Nanotechnology, Biology and Medicine, 2017.

18. Mano J F: Biomimetic approaches for biomaterials development, Wiley-VCH, Germany, 2013: 213-234.

19. Kim H N, Jiao A, Hwang N S, Kim M S, Kim D H, Suh K Y: Nanotopography-guided tissue engineering and regenerative medicine, Advanced Drug Delivery Reviews, 2013; 65(4): 536-558.

20. Kim D H, Lipke E A, Kim P, Cheong R, Thompson S, Delannoy M, Suh K Y, Tung L, Levchenko A: Nanoscale cues regulate the structure and function of macroscopic cardiac tissue constructs, Proceedings of the National Academy of Sciences 2010; 107(2): 565-570.

21. Topography, available (16.04.2018): https://www.google.si/search?safe=active&ei=PffWWsXnMqHcgAav9rLICw&btnG=Iskanje&q=topography+definition

22. Definition of topography, available (16.04.2018): https://www.collinsdictionary.com/dictionary/english/topography

23. Miller D C, Haberstroh K M, Webster T J: PLGA nanometer surface features manipulate fibronectin interactions for improved vascular cell adhesion, Journal of Biomedical Materials Research 2007; 81A: 678-684.

24. Biggs M J, Richards R G, Dalby M J: Nanotopographical modification: a regulator of cellular function through focal adhesions, Nanomedicine: Nanotechnology, Biology and Medicine 2010; 6(5): 619-633.

25. Simitzi C, Ranella A, Stratakis E: Controlling the morphology and outgrowth of nerve and neuroglial cells: The effect of surface topography, Acta Biomaterialia 2017.

26. Curtis A S G, Casey B, Gallagher J O, Pasqui D, Wood M A, Wilkinson C D W: Substratum nanotopography and the adhesion of biological cells, Biophysical Chemistry 2001; 94: 275-283.

27. Wójciak-Stothard B, Curtis A, Monaghan W, Macdonald K, Wilkinson C: Guidance and activation of murine macrophages by nanometric scale topography, Experimental Cell Research 1996; 223(2): 426-435.

28. Anselme K, Davidson P, Popa A M, Giazzon M, Liley M, Ploux: The interaction of cells and bacteria with surfaces structured at the nanometre scale, Acta Biomaterialia, 2010; 6(10): 3824-3846.

29. Dalby M J, Riehle M O, Sutherland D S, Agheli H, Curtis A S G: Changes in fibroblast morphology in response to nano-columns produced by colloidal lithography, Biomaterials 2004; 25: 5415-5422.

30. Yadav R K: Investing in nanotechnology, Mangalam Publishers, India, 2009: 72-84.

31. Rehfeldt F, Engler A J, Eckhardt A, Ahmed F, Discher D E: Cell responses to the mechanochemical microenvironment—implications for regenerative medicine and drug delivery, Advanced Drug Delivery Reviews 2007; 59(13): 1329-1339.

32. Khan S P, Auner G, Newaz G M: Influence of nanoscale surface roughness on neural cell attachment on silicon, Nanomedicine 2005;1, 125–129.

33. Fan Y W, Cui F Z, Hou S P, Xu Q Y, Chen L N, Lee I S: Culture of neural cells on silicon wafers with nano-scale surface topography, Journal of Neuroscience Methods 2002; 202: 17-23.

34. Gnavi S, Fornasari B E, Tonda-Turo C, Laurano R, Zanetti M, Ciardelli G, Geuna S: The effect of electrospun gelatin fibers alignment on Schwann cell and axon behavior and organization in the perspective of artificial nerve design, International Journal of Molecular Sciences 2015; 16, 12925–12942.

35. Loesberg W A, Te Riet J, van Delft F C, Schön P, Figdor C G, Speller S, van Loon J, Walboomers X F, Jansen J A: The threshold at which substrate nanogroove dimensions may influence fibroblast alignment and adhesion, Biomaterials 2007; 28(27): 3944-3951.

36. Teixeira A I, McKie G A, Foley J D, Bertics P J, Nealey P F, Murphy C J: The effect of environmental factors on the response of human corneal epithelial cells to nanoscale substrate topography, Biomaterials 2006; 27(21): 3945-3954.

37. Leor J, Gerecht S, Cohen S, Miller L, Holbova R, Ziskind A, Shachar M, Feinberg M S, Guetta E, Itskovitz-Eldor J: Human embryonic stem cell transplantation to repair the infracted myocardium, Heart 2007; 93(10): 1278-1284.

38. Cao H, Marcy G, Goh E L K, Wang F, Wang J, Chew S Y: The effects of nanofiber topography on astrocyte behavior and gene silencing efficiency, Macromolecular Bioscience 2012; 12, 666-674.

39. Zhang L, Webster T J: Poly-lactic-glycolic-acid surface nanotopographies selectively decrease breast adenocarcinoma cell functions, Nanotechnology 2012; 23 (15): 155101.

40. Popat K C, Leoni L, Grimes C A, Desai T A: Influence of engineered titania nanotubular surfaces on bone cells, Biomaterials 2007; 28(21): 3188-3197.

41. Dalby M J, Gadegaard N, Tare R, Andar A, Riehle M O, Herzyk P, Wilkinson C D, Oreffo R O: The control of human mesenchymal cell differentiation using nanoscale symmetry and disorder, Nature Materials 2007; 6(12): 997-1003.

42. Kantawong F, Burchmore R, Gadegaard N, Oreffo R O, Dalby M J: Proteomic analysis of human osteoprogenitor response to disordered nanotopography, Journal of the Royal Society Interface 2009; 6(40): 1075-1086.

43. Taubert A, Mano J F, Rodríguez-Cabello J C: Biomaterials surface science, Wiley-VCH, Germany, 2013: 89-528.

44. Wen X, Tresco P A: Effect of filament diameter and extracellular matrix molecule precoating on neurite outgrowth and Schwann cell behavior on multifilament entubulation

bridging device in vitro, Journal of Biomedical Materials Research Part A. 2006; 76(3): 626-637.

45. Xie J, Liu W, MacEwan M R, Bridgman PC, Xia Y: Neurite outgrowth on electrospun nanofibers with uniaxial alignment: the effects of fiber density, surface coating, and supporting substrate, ACS Nano 2014; 8(2): 1878-1885.

46. Rangappa N, Romero A, Nelson K D, Eberhart R C, Smith G M: Laminin-coated poly (L-lactide) filaments induce robust neurite growth while providing directional orientation, Journal of Biomedical Materials Research 2000; 51(4): 625-634.

47. Kim Y T, Haftel V K, Kumar S, Bellamkonda R V: The role of aligned polymer fiber-based constructs in the bridging of long peripheral nerve gaps, Biomaterials 2008; 29(21): 3117-3127.

48. Mukhatyar V J, Salmerón-Sánchez M, Rudra S, Mukhopadaya S, Barker T H, García A J, Bellamkonda R V: Role of fibronectin in topographical guidance of neurite extension on electrospun fibers, Biomaterials 2011; 32(16): 3958-3968.

49. Yuan Y, Zhang P, Yang Y, Wang X, Gu X: The interaction of Schwann cells with chitosan membranes and fibers in vitro, Biomaterials 2004; 25(18): 4273-4278.

50. Cecchini M, Bumma G, Serresi M, Beltram F: PC12 differentiation on biopolymer nanostructures, Nanotechnology 2007; 18(50): 505103.

51. Yao L, Wang S, Cui W, Sherlock R, O'Connell C, Damodaran G, Gorman A, Windebank A, Pandit A: Effect of functionalized micropatterned PLGA on guided neurite growth, Acta Biomaterialia 2009; 5(2): 580-588.

52. Gomez N, Lu Y, Chen S, Schmidt C E: Immobilized nerve growth factor and microtopography have distinct effects on polarization versus axon elongation in hippocampal cells in culture, Biomaterials 2007; 28(2): 271-284.

53. Li N, Folch A: Integration of topographical and biochemical cues by axons during growth on microfabricated 3-D substrates, Experimental Cell Research 2005; 311(2): 307-316.

54. Johansson F, Carlberg P, Danielsen N, Montelius L, Kanje M: Axonal outgrowth on nano-imprinted patterns, Biomaterials 2006; 27(8): 1251-1258.

55. Dowell-Mesfin N M, Abdul-Karim M A, Turner A M, Schanz S, Craighead H G, Roysam B, Turner J N, Shain W: Topographically modified surfaces affect orientation and growth of hippocampal neurons, Journal of Neural Engineering 2004; 1(2): 78.

56. Simitzi C, Stratakis E, Fotakis C, Athanassakis I, Ranella A: Microconical silicon structures influence NGF-induced PC12 cell morphology, Journal of Tissue Engineering and Regenerative Medicine 2015; 9(4): 424-434.

57. Simitzi C, Efstathopoulos P, Kourgiantaki A, Ranella A, Charalampopoulos I, Fotakis C, Athanassakis I, Stratakis E, Gravanis A: Laser fabricated discontinuous anisotropic microconical substrates as a new model scaffold to control the directionality of neuronal network outgrowth, Biomaterials 2015; 67: 115-128.

58. Haq F, Anandan V, Keith C, Zhang G: Neurite development in PC12 cells cultured on nanopillars and nanopores with sizes comparable with filopodia, International Journal of Nanomedicine; 2(1): 107.

59. Chapman C A, Chen H, Stamou M, Biener J, Biener M, Lein PJ, Seker E: Nanoporous gold as a neural interface coating: effects of topography, surface chemistry, and feature size, ACS Applied Materials & Interfaces 2015; 7(13): 7093-7100.

60. Kurtulus O, Seker E: Nanotopography effects on astrocyte attachment to nanoporous gold surfaces, InEngineering in Medicine and Biology Society (EMBC), Annual International Conference of the IEEE 2012, 6568-6571.

61. Biswas A, Bayer I S, Biris A S, Wang T, Dervishi E, Faupel F: Advances in top–down and bottom–up surface nanofabrication: Techniques, applications & future prospects, Advances in Colloid and Interface Science, 2012; 170(1-2): 2-27.

62. Puurunen R L: Surface chemistry of atomic layer deposition: A case study for the trimethylaluminum/water process, Journal of Applied Physics, 2005; 97(12): 9.

63. Nanoscience & Nanotechnology, Chemical Vapor Deposition, available (16.04.2018): https://sites.google.com/site/nanomodern/Home/CNT/syncnt/cvd

64. Sheikh I, Dahman Y: Applications of nanobiomaterials in hard tissue engineering, Nanobiomaterials in Hard Tissue Engineering, 2016: 57-58.

65. Multiphoton lithography, available (16.04.2018): https://ipfs.io/ipfs/QmXoypizjW3WknFiJnKLwHCnL72vedxjQkDDP1mXWo6uco/wiki/Multiphoton_lithography.html

66. Holographic lithography lecture, available (17.04.2018): https://www.youtube.com/watch?v=kPbEuGoMPfw

67. Santin M, Phillips G J: Biomimetic, bioresponsive and bioactive materials: An introduction to integrating materials with tissues, Wiley & Sons Inc., New Jersey, 2012: 198-202.

68. Eaton P, West P: Atomic force microscopy, Oxford University Press Inc., New York, 2010; 1-46.

69. Liu H, Webster T J. Nanomedicine for implants: a review of studies and necessary experimental tools, Biomaterials 2007; 28(2): 354-369.

70. Silicon wafer, what is it and what is it used for, available (23.04.2018): https://www.waferworld.com/silicon-wafer-what-is-it-and-what-is-it-used-for/

71. Yaşayan G, Xue X, Collier P, Clarke P, Alexander M R, Marlow M: The influence of nanotexturing of poly (lactic-co-glycolic acid) films upon human ovarian cancer cell attachment, Nanotechnology 2016; 27(25): 255102.

72. Guex A G, Fortunato G, Hegemann D, Tevaearai H T, Giraud M N: General protocol for the culture of cells on plasma-coated electrospun scaffolds, Stem Cell Nanotechnology: Methods and Protocols 2013; 119-131.

73. Rybczynski J, Ebels U, Giersig M: Large-scale, 2D arrays of magnetic nanoparticles, Colloids and Surfaces: Physicochemical and Engineering Aspects 2003; 219 (1-3), 1-6.

74. Baunack S, Zehe A: A study of UV/ozone cleaning procedure for silicon surfaces, Physica Status Solidi (a) 1989; 115.1: 223-227.

75. Bölgen N, Vargel I, Korkusuz P, Menceloğlu Y Z, Pişkin E: *In Vivo* Performance of Antibiotic Embedded Electrospun PCL Membranes for Prevention of Abdominal Adhesions, Journal of Biomedical Material Research 2007; 81B, 530–543.